Materials Advances

ROYAL SOCIETY OF CHEMISTRY

REVIEW

View Article Online
View Journal | View Issue

Cite this: *Mater. Adv.*, 2023, **4**, 726

A review on polymers and their composites for flexible electronics

Lixia Li,[abc] Lijing Han,[b] Haiqing Hu*[a] and Ruoyu Zhang*[b]

Flexible electronics have become an important trend in the information era. Consequently, the utilization of conventional metals and inorganic semiconductors is restricted in flexible devices due to their poor stretchability and adaptability. Thus, currently, it is urgent to find suitable candidates to at least partially replace these traditional components. In this case, polymers and their composites are considered as key materials for the fabrication of flexible electronic devices due to their excellent mechanical and electrical properties in flexible substrates, interfacial bonding, and functional active components. In this study, based on the important application value of polymers and their composites, non-functional materials such as substrate materials and adhesive materials, and functional materials including piezoelectric composites, conductive composites, and dielectric composites are summarized comprehensively. In addition, the structural features, performances, advantages, and disadvantages, as well as the main application scenarios of several common polymers are summarized in detail. Finally, we critically analyze the challenges and present future perspectives regarding polymers and composites for flexible electrics, aiming to realize their real applications.

Received 30th September 2022,
Accepted 16th December 2022

DOI: 10.1039/d2ma00940d

rsc.li/materials-advances

1 Introduction

With the rapid development of information technology such as 5G, the world is being rebuilt by digital technology. Accordingly, the way of manufacturing, living and exploring is changing deeply and significantly, and thus 'measurable' and 'digital' are needed everywhere. In this case, the traditional rigid electronic devices based on semiconductors, metals, and inorganic materials cannot satisfy the new requirements, such as flexibility, extendable and wearable.[1–6] Alternatively, flexible electronics have been booming in recent years because of their

[a] *Key Laboratory of Rubber-Plastics, Ministry of Education/Shandong Provincial Key Laboratory of Rubber-plastics, School of Polymer Science and Engineering, Qingdao University of Science and Technology, Qingdao, 266042, People's Republic of China. E-mail: hhq@qust.edu.cn*

[b] *Zhejiang International Scientific and Technological Cooperative Base of Biomedical Materials and Technology, Zhejiang Engineering Research Center for Biomedical Materials, Cixi Institute of Biomedical Engineering, Ningbo Institute of Materials Technology and Engineering, Chinese Academy of Sciences, Ningbo, 315300, People's Republic of China. E-mail: zhangruoy@nimte.ac.cn*

[c] *Department of Chemistry, Hengshui University, Hengshui, 053000, People's Republic of China*

Lixia Li

Lixia Li is currently a PhD scholar at the Qingdao University of Science and Technology, and is co-training at Ningbo Cixi Institute of Biomedical Engineering, Ningbo Institute of Materials Technology and Engineering, Chinese Academy of Sciences. She received her Master's Degree from Hebei University of Technology in 2012. Her area of interest focuses on the preparation of polyurethane and its application in flexible electronic devices.

Lijing Han

Lijing Han is a postdoc at Ningbo Cixi Institute of Biomedical Engineering, Ningbo Institute of Materials Technology and Engineering, Chinese Academy of Sciences, and her co-supervisor is Prof. Zhang. Her research currently focuses on the preparation of non-isocyanate polyurethane and its application in flexible electronic devices.

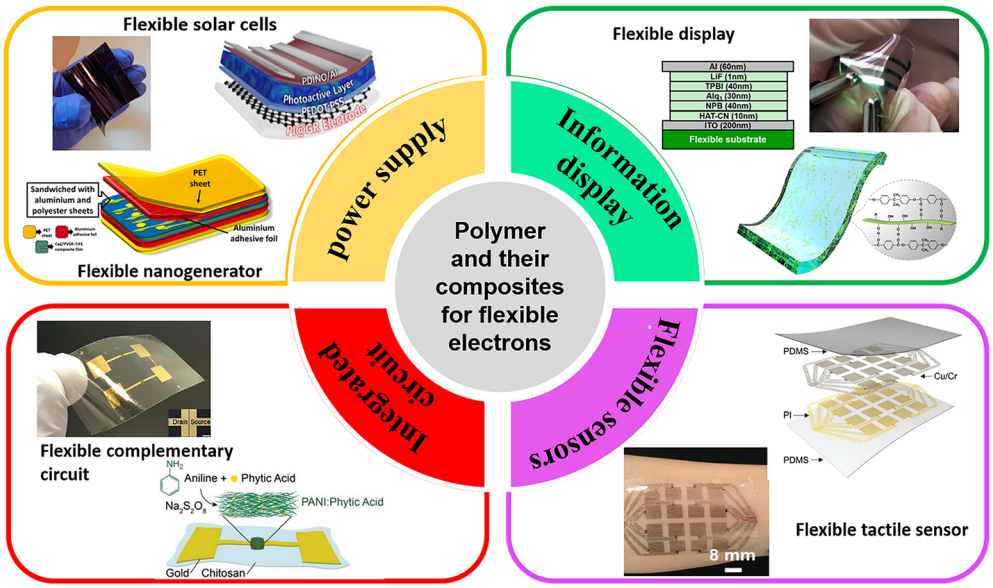

Fig. 1 Schematic of the applications of polymers and their composites in flexible electronics. Reproduced with permission ref. 3, 7, 17, 77, 78, 164 Copyright 2021, Elsevier; 2020, Elsevier; 2020, Elsevier; 2020, the American Chemistry Society; 2020, Wiley-VCH; and 2019, Wiley-VCH.

flexibility, wearability, and compatibility, showing great potential in energy collection, flexible displays, flexible sensor electronics, electronic skins, and many other fields. In these flexible devices, polymer materials play a very important role due to their versatile and adjustable properties including flexibility.[7–9] Firstly, compared to the traditional manufacture of electronic components, polymers can usually be processed by convenient and low-cost methods. Secondly, the chemical structures of polymers can be rationally designed to adapt to various applications. Thirdly, some polymers also have excellent biocompatibility and stability in the human body, endowing them with health monitoring capability in complicated biological conditions. Consequently, polymers have become one of the most indispensable materials in flexible electronics.[10–12]

To date, exciting achievements have been made in the area of flexible electronics. For the construction of full flexible sensor systems, at least four types of components are required, including a power supply, information display, interactive interface and integrated circuit, and a schematic of the applications of polymers and their composites in flexible electronics is shown in Fig. 1. Many researchers and companies are devoted to the development of these components. As a new type of green power supply, flexible solar cells have attracted significant attention in terms of flexible energy collection devices, which can be used in wearable electronic devices due to their

Haiqing Hu

Haiqing Hu received her PhD from the Institute of Chemistry, Chinese Academy of Sciences in 2005. After two years as a guest researcher at the National Institute of Standards and Technology, she joined Qingdao University of Science and Technology in 2008, and was promoted as a Full Professor in 2012. Her current research focuses on the fundamental understanding of polymer materials from a physical–chemical point of view.

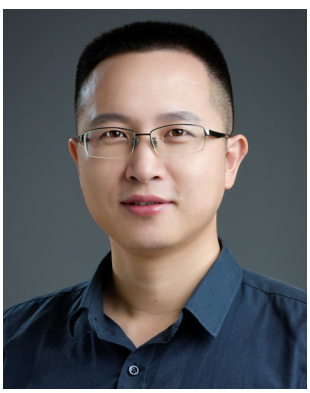

Ruoyu Zhang

Prof. Ruoyu Zhang obtained his PhD from the Institute of Chemistry, Chinese Academy of Sciences, focusing on phase separation in polymeric blends. He spent almost three years as a Post-doc in California Institute of Technology, where he continued his research on crystallization. In 2011, he joined Ningbo Institute of Materials Technology and Engineering, Chinese Academy of Sciences. Subsequently, he turned his research interest to the multi-scale structure of thermoplastic polyurethanes and the development of high-performance and functional polyurethanes in flexible electronics and medical devices.

flexibility and portability. Professor Takao Someya's team made an outstanding contribution to the field of flexible solar cells. Recently, they proposed the concept of bendable ultra-thin solar cells using transparent polyimide (PI) as the substrate with a thickness of only 1.3 μm. Due to their good adaptability and tensile capacity, these ultra-thin organic solar cells show great application prospects.[13] Another type of important energy device is flexible nanogenerators. Utilizing the piezoelectric properties and semiconductor coupling effect of ZnO nanowires (ZnONWs), Professor Zhonglin Wang's research group successfully converted mechanical energy into electrical energy and developed the world's smallest generator, a piezoelectric nanogenerator, for the first time.[14–17] In 2012, polyethylene terephthalate (PET) and PI films with different friction characteristics were assembled into the first friction-type nanogenerator, which effectively improved the electromechanical conversion efficiency and electrical output of the device,[14] and the relevant research reports have attracted wide attention from researchers in many areas.[15,17,18] Similar to the field of flexible displays, the current mainstream is flexible organic light-emitting diode (OLED) technology, among which active-matrix organic light-emitting diode (AMOLED) displays have become one of the hottest research directions in the field of consumer electronics in the last decade.[19] Currently, foldable AMOLED mobile phones represented by Huawei's Mate X series and Samsung's Galaxy Fold series have gone into mass production and become very attractive consumer electronic products.[20–22] Furthermore, in the case of soft sensing, many research groups and companies have achieved significant progress. For example, Prof. Zhenan Bao's group has made outstanding achievements.[23–25] For instance, they reported the preparation of an electronic skin based on an anion conductor, 1-ethyl-3-methylimidazolium bis(trifluoromethylsulfonyl)imide (EMIM TFSI), which was spin-coated on a stretchable composite electrode film made with Ag nanowires and polystyrene-*block*-poly(ethylene butylene)-block polystyrene (SEBS). This flexible sensor could simultaneously respond to temperature and stress, and it behaved as electronic skin that could feel warm and tactile like human skin. This electronic skin combined complex functions with related simple construction, which is a milestone in this field.[26] Lastly, although the development of flexible devices is noteworthy, integrated circuits are also essential. John A. Rogers's group firstly manufactured a flexible complementary inverter circuit using low-cost, low-temperature casting and micro-contact printing techniques on a plastic substrate.[27] Thus far, significant progress has been made in flexible complementary circuits operating at low voltages, which have low power consumption and high noise margin.[28]

Although polymeric materials show many advantages including flexibility, conformality, and wearable portability, these organic materials still have obvious disadvantages compared with inorganic semiconductors and metal conductors in terms of electrical properties and device stability. Although the power conversion efficiency (PCE) of flexible solar cells has exceeded 19%,[29] it is still far lower than that of rigid solar cells.[30,31] The energy collection output power of flexible nanogenerators is in the range of milliwatts,[32] which can only drive low-cost electronic equipment.[33,34] Thus, it is necessary to further improve the energy conversion efficiency and output voltage capacity of piezoelectric polymers. Next, transparent plastic substrates such as PI and PET in flexible display devices all belong to non-crosslinked polymer materials from the viewpoint of molecular architecture. The chain segments and long chains of these non-crosslinked polymer move slowly under external stress, leading to the creep phenomenon, which affects the appearance, feel and service life of the folded display product.[21] Besides the creep resistance property, the long-term light transmittance, surface finish and thermal stability of the polymeric matrix need to be further improved to narrow the gap with inorganic glass. The flexible sensing area also faces some challenges, in which the core issue is how to balance the sensitivity and sensing strain range of the sensing material. The key to solve this problem is to choose suitable materials, and among the commonly used materials, conductive polymer composites are outstanding candidates for the flexible strain sensors because of their high mechanical durability, large strain tolerance and adjustable nature.[35–37] It has been reported that conductive composites can achieve a high sensing performance through multi-scale structural designs, such as the preparation of double percolation network structures,[38] isolation structures,[39] and porous structures.[40,41] Nevertheless, there are still many challenges such as high sensitivity in a low sensing range and large sensing range with low sensitivity. Another practical problem is that the interface layer can be mismatched between the functional active material and the flexible substrate material during the use of flexible electronic devices, which can lead to the failure of device and affect its service life. In recent years, mussel-inspired hydrogel adhesives have aroused great interest among scientists, where the operating stability and durability of the overall devices can be improved by adopting these polymers.[11,42,43] In the case of flexible complementary circuits, there many organic complementary circuits have been reported,[44–46] but few studies have been done on flexible substrates to demonstrate fully printed complementary technologies with both high mobility P-type and N-type semiconductors. Briefly, with the increasing demand for flexible electronic products, it is urgent to develop integrated and multi-functional electronic devices, which requires the incorporation of materials science and other disciplines, such as life sciences, machinery, and electronics.

Based on the above discussion, it is known that polymers and their composites have been widely used as non-functional materials such as flexible substrates, adhesive materials, and functional materials such as sensor elements, electrodes, and piezoelectric elements. Considering the great achievement and the existing challenges in polymer-based flexible electronics, it is necessary to review the development of polymers and their composites used in the field of flexible electronics and to provide a reference for researchers in related fields. In this work, several important application directions in flexible devices including solar cells, nanogenerators, displays and

sensing are summarized. Furthermore, both non-functional and functional materials including matrix, adhesive materials, conductive composites, piezoelectric composites and dielectric blends are extensively discussed, and the advantages and disadvantages of these candidates are also analyzed. Finally, the existing problems and challenges are presented and the possible methods are proposed.

2 Overview of flexible components

2.1 Flexible energy collection devices

2.1.1 Flexible solar cells. The newly emerging flexible solar cells have become a research hotspot due to their compatibility wearable electronic systems such as electronic textiles and synthetic skin in everyday life.[47–50] The typical structures of the flexible solar cells adopting soft, light-weight and plastic polymer substrates are shown in Fig. 2a. Moreover, these polymer matrixes are also highly transparent and feasible to be processed, which can be manufactured on a large scale using techniques such as continuous roll-to-roll procedure.[47,51] Considering their high temperature resistance, low cost, and good recyclability, PET, polyethylene naphthalene (PEN) and PI-containing aromatic structures are the most widely reported polymer substrates.[52–56] To replace the traditional indium tin oxide (ITO),[57] conductive polymeric composites containing metal nanowires, graphene and carbon nanotubes (CNTs) have been evaluated.[58–61] Alternatively, the conductive polymer poly(3,4-ethylene dioxythiophene): styrene sulfonate (PEDOT: PSS) with inherent flexibility has been widely used in recent years due to its low price, excellent transparency, high conductivity, and good solution processing performance.[62] Song *et al.*[63] reported a new method using PEDOT: PSS as an electrode for the fabrication of a flexible organic solar cell (OSC) with a maximum power conversion efficiency of 10.12%, bringing flexible OSCs closer to commercialization.

2.1.2 Flexible nanogenerators. Because the normal battery has a limited capacity,[64,65] researchers have developed nanogenerators, which can harvest energy during *in vivo* and/or *in vitro* human movement.[66–68] Flexible nanogenerators mainly include piezoelectric nanogenerators (TPNG) and triboelectric nanogenerators (TENG), in which mechanical and frictional energy are converted into electrical energy,[68] respectively. A schematic diagram of a flexible piezoelectric nanogenerator is shown in Fig. 2b, which has two electrodes covering the top and bottom of the insulated piezoelectric material. In the case of triboelectric nanogenerators, a diagram of their structure is shown in Fig. 2b. The negative tribo-material with strong electronegativity and the positive tribo-material with weak electronegativity act as two different triboelectric layers and the two layers connect the two electrodes separately.[69] In these nanogenerators, the main parameters evaluating their performance include output voltage, output power and device stability,[70,71] and the focus is usually how to improve and optimize the electrical output efficiency of the devices.

2.2 Flexible displays

Flexible displays are expected to be thin, light and endure repeatable bending, folding, curling and even stretching. The current mainstream product is the flexible OLEDs.[72] OLEDs are stacked on a glass substrate in a specific form and encapsulated with glass or metal plate as in the traditional LED display,[73] and a diagram of their structure is shown in

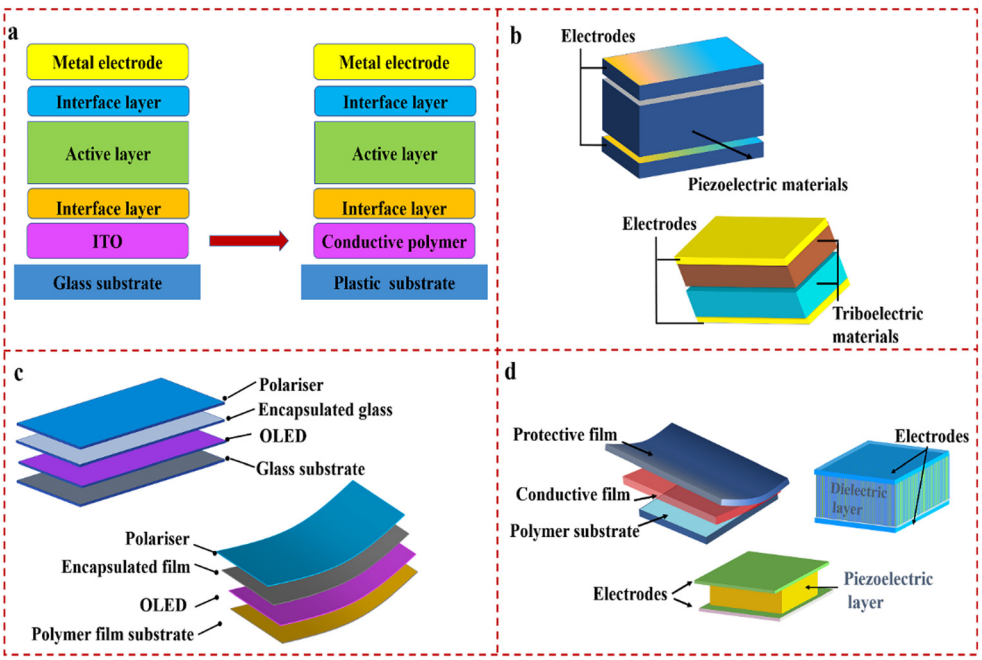

Fig. 2 (a) Typical structure of organic solar cell intentions. (b) Typical structure of a TPNG and TENG. (c) Typical structure of an ordinary display and flexible display. (d) Structure of a resistive sensor, piezoelectric sensor and capacitive pressure sensor.

Fig. 2c. Compared with the traditional displays, the glass substrate is replaced by a thin and light plastic film in a flexible OLED screen, as shown in Fig. 2c. Currently, flexible OLED screen technology is considered to be one of the most promising next-generation display technologies,[74] which can be widely used in consumer electronics such as mobile phones, TVs, wearable devices and vehicle-mounted displays.

The flexible plastic film used for the flexible display exhibits reasonable trade-offs in mechanical, optical, and chemical properties, which can be produced by a roll-to-roll process and adapt to high-temperature processing technology.[75–77] Nevertheless, compared with inorganic glass, common plastic substrate materials have inferior transparency, high thermal expansion coefficient (CTE),[78] permeability to water and oxygen, and easily deformed, which affect the service life of the display, and thus it is necessary to design the molecular structure to improve performance of the polymers and ameliorate technological processes to overcome the existing problems for meeting the increasing demands in society.

2.3 Flexible sensing

Flexible sensors are one of the main forms of flexible electronics, which have become a research hotspot due to their unique advantages such as high sensitivity, durability and biocompatibility.[79–81] Strain sensors can be mainly divided into three types, *i.e.*, resistive, capacitive and piezoelectric sensors. Among them, the typical structure of resistive strain sensors contains a conductive film coupled with a flexible substrate, as shown in Fig. 2d. Their basic working principle is that the resistance changes with the deformation of the sensing material, which is reflected as the corresponding change in electrical signal. The core structure of a capacitive sensor is the parallel plate capacitance, as shown in Fig. 2d, which is composed of a dielectric layer in the middle and two parallel electrodes on the two sides. Its basic working principle is that mechanical deformation induced by external stress causes a distance change between the two electrodes, resulting in a variation in capacitance. Compared with resistive and capacitive sensors, piezoelectric pressure sensors are mainly composed of upper and lower electrodes and a middle layer of piezoelectric materials, as illustrated in Fig. 2d, and their working principle is based on the piezoelectric effect.[68] When a dielectric material is deformed by external pressure, it will generate internal polarization and an internal electric field, and then an electrical voltage is generated between the two electrodes. The charge is proportional to the applied pressure, which will disappear when the external force is removed.

2.4 Flexible complementary circuits

Flexible complementary circuits are widely used in electronic fields, demanding energy supply/dissipation requirements. The typical structure of a flexible complementary circuit includes a P-type and N-type organic thin film transistor (OTFT). The basic working principle is to select the working gate input range to enable only one transistor to be ''on'', while the other is ''off''. Consequently, the complementary circuits have the advantage of reducing the power consumption by keeping one of the two devices off.[44]

Polymers can play an incomparable role in flexible complementary circuits. Firstly, as the channel layer of OTFT, compared with inorganic and metal oxide semiconductors, conjugated polymers have great advantages in flexibility and solution-processability. Secondly, OTFTs are generally manufactured on polymer substrates because of their broad fabrication methods and excellent flexibility, and their performance is similar to that of devices on silicon substrates without significant attenuation. Lastly, some relatively high molecular weight polymers, such as polystyrene (PS), polymethyl methacrylate (PMMA), PI, and polyvinyl alcohol (PVA) have been used as an organic insulation layer on account of their advantages of solution processing and preparation of ultra-thin films.[82]

3 Non-functional polymer materials in flexible electronics

Non-functional polymer materials mainly include polymer substrates and adhesive materials. In flexible electronic devices, the active electronic components, whether made of organic, inorganic or hybrid materials, are usually constructed on polymer substrates. Polymer substrates with flexibility/malleability, suitable modulus and insulation not only can play a supporting role, but more importantly, directly determine the flexibility of electronic devices. In addition to polymer substrates, polymer adhesives have been widely used in flexible devices due to their advantages of low cost, simple preparation process, and outstanding bonding effect, which can significantly improve the operating stability and durability of flexible instruments.

3.1 Flexible substrates

Plastic and elastomeric substrates are the two most widely used flexible substrates, in which plastic substrates such as PI, PET, and PEN are mainly used in the fields of flexible solar cells and flexible displays. As the supporting matrix, they are required to have good insulation, high strength, excellent bending property, good transparency and temperature resistance. However, in recent years, with the fast development of wearable strain sensors, electronic skins, flexible biomedical devices and flexible electronic devices, plastic substrates cannot satisfy the requirement of free movement.[8,9,83] Consequently, elastomeric substrates with high stretchability and elasticity offer the opportunity to address this challenge, and they have become the preferred materials in the above-mentioned applications. The typical elastomers are PDMS and thermoplastic polyurethane (TPU). Table 1 presents a summary of the most common polymer substrates, including their thermal and mechanical properties.

3.1.1 PET substrates. PET is a commercialized and recyclable semicrystalline thermoplastic polymer with good toughness, high transmittance in the visible light range, relatively low gas and water vapor permeability, and acceptable chemical resistance. Thus, it is widely used in flexible solar cells, flexible

Table 1 The properties of common polymer substrate materials

Substrate	T_g (°C)	Elongation at break (%)	Young's modulus (MPa)	T_{max} (%)	Applications	Ref.
PET	68–71	1.5–4.0	2000–5300	80–90	Flexible displays, flexible organic solar cells, gas sensing	50, 79, 84
PI	>400	8.74	2800–4500	90	Flexible organic solar cells, flexible displays	78, 86
PDMS	−128 to −123	200	0.5–3	87	Strain sensors	87, 88
TPU	−32 to −71	500–900	17–27	80	Strain sensors, capacitive sensors	89

displays and many other fields. Heeger's research group[90] reported the fabrication of a flexible OLED for the first time. They used a polyaniline (PAN) or PAN mixture to form a conductive film on a PET substrate *via* the spin-coating method as a transparent anode of the OLED device, which paved the way for the development of flexible displays of OLEDs. The preparation of flexible organic solar and complementary circuits on PET substrates has also been widely reported.[27,50,78,91–93]

However, the low surface free energy of PET causes difficulty in wettability, adhesion and printability. Thus, various methods have been adopted for the surface modification of PET films, such as chemical modification, heat treatment and plasma treatment.[94–96] For example, Chang *et al.*[97] treated a PET film with oxygen plasma to generate active spots on its surface. Moreover, electronic and optoelectronic devices require ultra-clean and smooth surfaces. Zhang and co-authors[85] modified the surface of PET using a mild treatment with a moderate acid concentration of a mixture of sulfuric acid and hydrogen peroxide at room temperature. The surface smoothness of PET was significantly improved after this treatment, as shown in Fig. 3a and b. Another challenge associated with PET substrates is their thermal instability. The glass-transition temperature (T_g) of PET is about 71 °C, and its CTE value is 20–80 ppm K^{-1}, which is greater than that of inorganic glass.[78] Consequently, they are vulnerable to damage during manufacturing.

3.1.2 PI substrates. Due to the aromatic heterocyclic conjugated effect, PI with aromatic heterocyclic moieties has strong molecular inter-atomic forces, making its molecular chain rigid. PI possesses excellent chemical stability, mechanical properties, and good heat resistance, which can resist temperatures as high as 400 °C or above and endure for a long time at 200–300 °C with low thermal expansion coefficient.

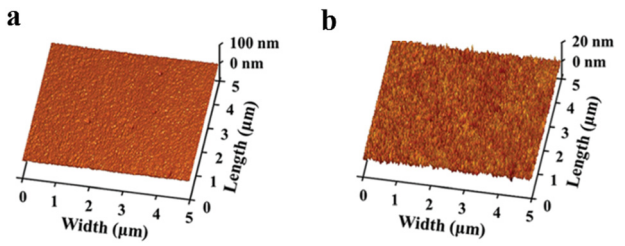

Fig. 3 (a) AFM image of the pristine commercial PET substrate. (b) AFM image of PET substrate after smoothing treatment. Reproduced with permission ref. 85. Copyright 2021, The Royal Society of Chemistry.

Traditional PI films have strong intramolecular and intermolecular charge transfer complexes (CTCs) because of their highly conjugated molecular structure, which causes strong light absorption in the ultraviolet-visible light range, making the film look yellow or brown. Thus, to expand the application of PI, the development of colorless polyimide (CPI) has become a research hotspot. According to the literature, CPI can be synthesized by adding flexible or asymmetrical bonds in the main chain of PI, introducing kinks, helices, and bulky or dangling substituents, and using aromatic fluorinated monomers.[77,98,99] CPI not only maintains excellent heat resistance but also has highly visible light transmittance, which can be used in fully transparent flexible displays and organic solar cells.[100] Chen *et al.*[101] synthesized a CPI using *trans*-1,4-cyclohexyl diamine,3,3,4,4-biphenyl tetracarboxylic anhydride and phthalic anhydride. They prepared flexible OFET devices with CPIs as substrates and proved that they had ultra-low CTE and sufficient mechanical durability, which maintained a good performance after 1000 bending cycles and high-temperature heating tests. Someya's group[13] reported the fabrication of thin and flexible solar cells using CPI as the substrate, which had a thickness of only 1.3 μm. This reduced thickness endowed the organic solar cells with excellent flexibility, which may find great applications in self-powered wearable electronics and soft robots. CPI not only possesses high mechanical stability, but also high adhesion strength with conductive active materials, such as silver nanowires (AgNWs) and CVD-grown graphene. Furthermore, it is an effective strategy to embed conductive materials in substrates to improve their interfacial adhesion.[49,102]

3.1.3 PDMS substrates. PDMS is a type of excellent elastomer with elongation of up to 160–180% and has good thermal stability, which can be used for a long time at 150 °C.[103] Importantly, PDMS has excellent transparency and biocompatibility and can be easily built into various structures with the assistance of templates. However, the adhesion of PDMS with other active materials is poor due to its low surface energy. In this case, chemical modification and surficial design of PDMS are used to improve its adhesive strength. For example, Byeongkwon Ju *et al.*[104] sandwiched AgNWs on a PDMS substrate using polyurethane urea (PUU) as the top layer, which contains 2,2-bis(hydroxymethyl) butyric acid. Inspired by the Lotus leaf, Huang *et al.*[105] prepared a bionic elastomer microporous film (BEMF) with uniformly distributed micropores *via* a one-step soft photolithography copying process and modified the PDMS substrate with dopamine and functionalized silane. In addition,

PDMS has high permeability to oxygen and water vapor, making it ideal for the fabrication of wearable and implantable devices. However, its high permeability prevents its application in electronics such as OLEDs, light-emitting electrochemical cells (LEECs) and organic photovoltaic devices (OPVs).[106]

3.1.4 TPU substrates. TPU is a block copolymer obtained *via* the addition polymerization of macromolecule polyester or polyether polyol, chain extender and diisocyanate. The carbamate group-based hard segment and polyol-based soft segment (polyol) can form a "microphase separation" structure, which endow TPU with excellent elasticity and flexibility, good chemical stability, biocompatibility, and outstanding wear and corrosion resistance. The performances of TPU can be optimized by adjusting the type and proportion of polyol (ether) and diisocyanate, which make TPU one of the most important candidates for the fabrication of wearable pressure sensors and intelligent instruments.[80,107,108] For example, Behfar *et al.*[109] directly printed circuit boards and assembled components through a roll-to-roll process on a TPU thin film and evaluated the device performance by controlling uniaxial cyclic strain at 5% and 10% elongation, and the durability tests showed that the assembled equipment could maintain their function after hundreds of deformation cycles. Nevertheless, stress relaxation is the main challenge associated with the use of TPU, which can cause fatigue and failure in the flexible devices. The reason for stress relaxation is that the hard segment phase, which is the physical crosslinking point, is damaged when subjected to a large external force. Recently, Prof. Ruoyu Zhang's group[110] introduced a cyclohexane ring in the soft segment of TPU (Fig. 4a) to improve its stress-relaxation and fatigue resistance. Consequently, even after 20 h of fixation under 300% strain and 1000 cycles of stretching (50% strain), the recovery rate was still higher than 98% (Fig. 4b and c). Another problem is its low thermal stability, which inhibits its application in organic solar cells and photovoltaic devices. In this case, the functionalization of TPU flexible substrates can endow them with self-healing, superhydrophobic, biodegradable and other functions through molecular design, and also enable the synthesis of eco-friendly biocompatible polyurethanes by replacing isocyanates with non-isocyanates,[111–113] which will play a pivotal role in future flexible electronic applications.

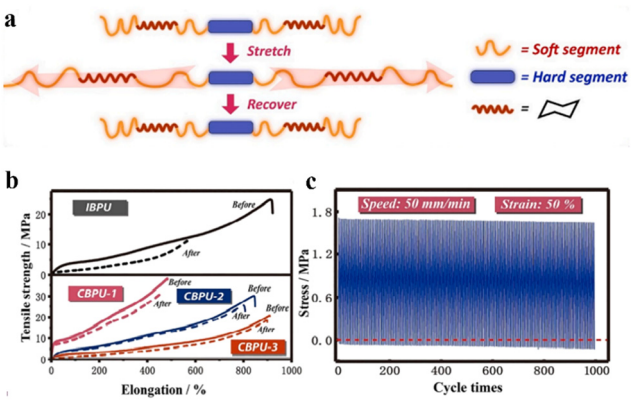

Fig. 4 (a) Schematic of the conformational variation of the soft segment and cyclohexane ring under tensile stress. (b) Strain–stress curves of IBPU. (c) Anti-fungal tests and cyclic tensile test of CBPU-3 at 50% strain for 1000 cycles. Reproduced with permission from ref. 110. Copyright 2020, Elsevier.

3.2 Polymeric adhesives

Tight bonding between functional components and flexible substrates is required to ensure device stability and long service life. However, different components have very different mechanical and surficial properties.[114] Thus, finding polymeric adhesives that have excellent adhesion strength through chemical bonds is also crucial in flexible devices (covalent bonds, ionic bonds, action of hydrogen bonding, *etc.*).

Polyurethane, PDMS, hydrogels, epoxy resins and polyacrylic esters are the main species of polymeric adhesives. Wong *et al.*[115] developed a polyurethane-based conductive adhesive (PU-ECA) and tested its adhesive strength to paper, PET and PI substrates. The results showed that the PU-ECA layer strongly adhered to flexible substrates and could resist the easement of a commercial tape. Yu *et al.*[116] reported the preparation of a printable tough hydrogel binder in one step using commercial chemicals, where its strong adhesion comes from three orthogonal photochemical reactions (Fig. 5a). It showed excellent adhesion and anti-fatigue capability on different surfaces, and was not sensitive to water, even when submerged under water. Jiang *et al.*[117] developed a high-performance adhesive for combining rigid electronics and deformable circuits based on PDMS elastomer and carbon nanotube/liquid metal co-filler. This conformable adhesive exhibited strong adhesion to the polymer substrate and conductive stability. Compared with the above-mentioned polymer adhesives, epoxy resins and polyacrylic esters have rarely been used due to their rigidity and high hardness.

In recent years, inspired by the excellent adhesive properties of marine biological mussels, the study of mussel-inspired adhesives and their applications in flexible electronic devices has attracted wide attention. The foot protein in mussels contains abundant dopamine molecules, which can form thin polydopamine (PDA) coatings on a variety of inorganic and organic materials through polymerization reactions, including intermolecular polymerization and intramolecular polymerization. Fu *et al.*[118] realized strong bonding between AgNW and hydrophobic substrates by adopting PDA-functionalized nanofiber (PDA@NFC) and successfully assembled a double-layer transparent and conductive cellulose-based nanopaper (TCCNP) with good mechanical and chemical stability. Even after 1000 bending cycles and 100 stripping tests, the changes in its photoelectric properties were negligible, implying the stability of the adhesive layer. To date, as a stable binder, PDA has attracted much attention due to its arbitrary deposition capacity and long-term stability. In addition, PDA is considered to be a promising candidate for the design of novel flexible bioelectronic devices with unique contributions both in structure and functionality. Li *et al.*[119] prepared a novel color film with a stretchable, adherent and conductive structure by adding conductive carbon nanotubes/PDA filler to PU reverse opal scaffolds (Fig. 5b and c). The catechol groups on PDA endowed

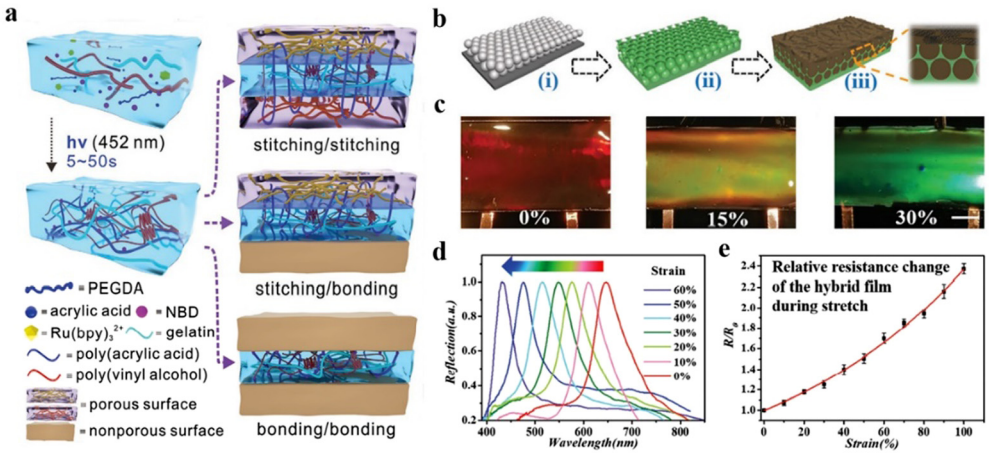

Fig. 5 (a) Schematic of preparation of tough multinetwork PTA based on orthogonal Ru(II)/NBD photochemistry. Reproduced with permission from ref. 116. Copyright 2022, Wiley-VCH. (b) Scheme and microstructures of hybrid films. (c) Optical images of the structural color changes of hydrogel hybrid under different strains. (d) Relationship between the reflectance wavelength and stretching intensity. (e) Relative resistance changes of the stretched film. Reproduced with permission from ref. 119. Copyright 2020, Wiley-VCH.

the film with high tissue adhesion and self-healing ability. Notably, due to its responsiveness, the synthesized film could change color in response to motion and be used as a dual-signal soft human motion sensor for real-time color perception and electrical signal monitoring (Fig. 5d).

4 Functional polymeric composites in flexible electronics

Functional polymeric composites in flexible electronics mainly include piezoelectric composites, conductive composites and dielectric composites. Piezoelectric composites can be used as piezoelectric sensors, energy collection and self-powered electron nanogenerators.[2,33,120] Conductive composites are potential candidates as strain sensors, which can monitor the strain variation based on resistance change.[121] Dielectric composites, incorporating inorganic/organic fillers in the micro/nanometer range with high dielectric constant or polarizability, possess cohesiveness, toughness and workability, as well as high dielectric properties.[122–124] Table 2 presents a summary of the methods for the preparation of functional polymer composites and their applications.

4.1 Polymeric piezoelectrics

Polymeric piezoelectric materials have found wide application in energy collection devices and self-powered sensors. PVDF

Table 2 The various reported polymer composites and their processing techniques and applications

Polymer matrix	Functional filler	Processing technique	Application	Ref.
PDMS	MWCNT	Solution casting	Resistive sensor	125
PDMS	Graphene Oxide	Casting	Strain sensor	126
PDMS	$BaTiO_3$/MWCNT	Solution casting	TENG	127
PDMS	Ag-CNTs-rGO	Template method	Resistive sensor	128
PDMS	Carbon black	Solution casting	Capacitive sensor	129
PDMS	ZnO	Solution casting	Piezoelectric sensor	130
TPU	Carbon black	3D printing	Strain and tactile sensors	131
TPU	SWCNT/rGO	Dip-coating process	Strain sensor	132
TPU	AgNWs/rGO	Electrospinning and Spraying alternately	TENG	133
TPU	CNS/GNP	Melt processed	Capacitive sensor	134
SBS	MWCNT	Wet-spinning	Strain sensor	135
SBS	Graphene	Wet-spinning	Piezoresistive strain sensor	136
SBS	Ag–Au	Solution casting	Biosensing	137
SBS	Ag nanoparticles	Electrospinning and situ self-assembly	Electric circuits	138
PVDF	CNT	Solution mixed	PENG	139
PVDF	Graphene nanoplatelets	Solution casting	Strain sensor	140
PVDF	Layered double hydroxides	Spin coating	TENG	141
PVDF	$CsPbBr_3$	Electrospinning	PENG	70
PVDF-HFP	$(BaCa)(ZrTi)O_3$	Electrospinning	PTNG	17
PVDF-HFP	$BaTiO_3$	Solution casting	PENG	1
PVDF-HFP	ZnO	Electrospinning	Strain sensor	142
PVDF-TrFE	rGO	Solution mixed and situ polarization	PENG	143
PVDF-TrFE	Pb $(Zr,Ti)O_3$	Spin coating	PENG	71
PVDF-TrFE	MXene	Electrospinning	TENG	144

and its copolymer, poly(vinylidene fluoride-trifluoroethylene) (P(VDF-TrFE)) and poly(vinylidene fluoride-hexafluoropropylene) (P(VDF-HFP)) are the most commonly used polymers. However, it is difficult for single polymeric piezoelectric materials to meet the requirements of high piezoelectric properties, and thus the introduction of proper fillers becomes inevitable. Besides PVDF and its copolymer, PDMS, PVC, PU, *etc.* have also been used in the preparation of piezoelectric composites.

4.1.1 PVDF-based piezoelectrics. PVDF has good mechanical toughness, chemical stability, and biocompatibility and has been widely used in the fields of flexible wearable piezoelectric sensors and nano-piezoelectric generators. It is a semi-crystal polymer with the crystal structure of 5 different lattice forms (α, β, γ, δ, and ε). The main chain conformation in the β phase of PVDF is the all-*trans* conformation and its polarization intensity is the highest among its 5 crystal forms with a piezoelectric coefficient of -29 pm V^{-1}. Given that the PVDF crystal is usually in the α phase, it is necessary to transform the α phase into β phase with higher piezoelectric coefficient. However, compared with inorganic ceramic materials, the piezoelectric coefficient of PVDF is still low. In this case, by introducing CNTs, graphene, ZnO, and barium titanate (BTO) nanoparticles in the PVDF matrix, β nucleation can be effectively promoted and its piezoelectric properties can be improved siginificantly.[67,70,142,145]

PVDF-based piezoelectrics combine the advantages of high piezoelectric coefficient of inorganic fillers and the flexibility of PVDF. Generally, these piezoelectric composites can be prepared *via* melt blending and solution blending, and an external electric field can improve the piezoelectricity of PVDF films. For example, Zhu *et al.*[146] prepared BTO-PVDF/GO core–shell piezoelectric nanofibers with PVDF/GO as the sheath and PVDF/BTO as the core *via* a coaxial electrostatic spinning process (Fig. 6a). Electron microscopy (Fig. 6b) showed that BTO nanoparticles (NPs) and GO nanosheets were introduced in the core shell of the composite nanofibers, which effectively enhanced the piezoelectric response and polarization effect. The resulting electronic skin (Fig. 6c) was sensitive in the pressure range of 80–230 kPa with sensitivity of up to 10.89 mV kPa^{-1} (Fig. 6d) and it could withstand 8500 consecutive operations. In another example, Asadi *et al.*[67] prepared PVDF nanofibers *via* electrostatic spinning. The hybrid nanofillers were composed of ZnO and reduced graphene oxide (rGO), and the ZnO-modified rGO flakes were doped with PVDF nanofibers. Large rGO flakes are flexible and can be folded inside the fibers to form bead structures (Fig. 6e). By optimizing the amount of hybrid filler, only 0.1% wt% ZnO: rGO hybrid filler was added when the mass ratio was 90 : 10. The output voltage of the nanogenerator prepared by the PVDF nanocomposite fiber was nearly 10-times (Fig. 6f) higher than that of previous PVDF nanocomposite fibers. The PVDF piezoelectric composite nanogenerator was applied to a battery-free cardiac pacemaker, which successfully collected 0.487 μJ (Fig. 6g) of energy per heartbeat, which is much higher than the pacing threshold of the human heart.

4.1.2 P(VDF-TrFE) piezoelectric composites. By introducing –CHF–CF$_2$– segments in the main chain of PTFE, we can obtain the copolymer of P(VDF-TrFE) with enhanced capability in forming β-phase crystals. When the content of TrFE exceeds a certain amount, the relatively high rotational barrier between

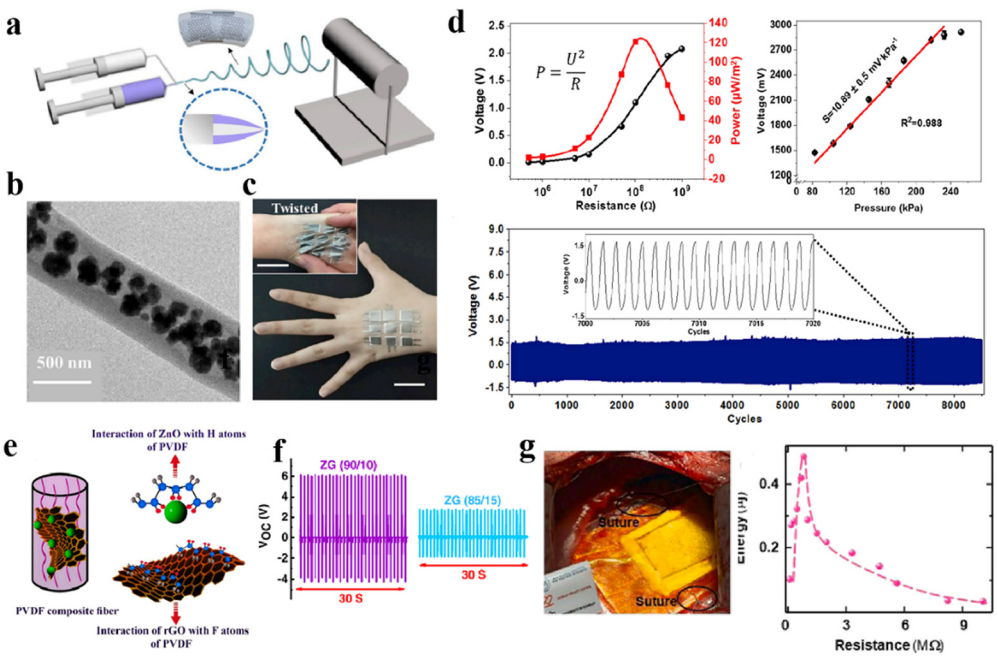

Fig. 6 (a) Schematic of the experimental setup for the coaxial electrostatic spinning process. (b) TEM image of a core–shell piezoelectric nanofiber. (c) Optical photograph of electronic skin attached on the back of the hand. (d) Performances of output voltage and sensing stability test. Reproduced with permission from ref. 146. Copyright 2020, Elsevier. (e) Schematic representing dispersion of hybrid nanofillers inside PVDF NFs. (f) VOC values of PNGs. (g) PNG sutured on the epicardium facing the lateral wall of LV (left) and the generated energy of PNG measured across a range of load resistances (right). Reproduced with permission from ref. 67. Copyright 2021, Elsevier.

–CHF–CF_2– and –CH_2–CF_2– suppresses the conformation of *trans*-torsional. Consequently, the P(VDF-TrFE) product is formed with a high β-phase content. Alternatively, it has been found that the addition of ZnO, piezoelectric ceramics, metal nanoparticles, and graphene can effectively improve the piezoelectric properties of P(VDF-TrFE). For example, Sahoo *et al.*[147] synthesized calcium-doped ZnO (CaZ) nanoparticles *via* chemical coprecipitation and the solution-casted CaZ/P(VDF-TrFE) composite films were used as the active layer of a piezoelectric energy capture device. In the continuous finger tapping mode, the rectification voltage response of the composite film reached 3 V, whereas under the action of 0.5 N oscillation force, the maximum output voltage of the device was 0.289 V.

P(VDF-TrFE) also has excellent spinning ability, where the heat generated in the electrostatic spinning process and the larger charge flow lead to polymer chain stretching, resulting in an α- to β-phase transformation, without any post-treatment.[148] Shao *et al.*[149] developed novel P(VDF-TrFE) based electrospinning nanofibers with rGO and loaded MWCNTs, which could be used to manufacture ultra-sensitive piezoelectric pressure sensors. When the content of RGO-MWCNTs as the dopant was 3.2%, the β phase increased to 92% (Fig. 7a). P(VDF-TrFE) nanofibers have high thermal stability due to the increase in their crystallinity. In the variable applied pressure range of 0.25–300 cN, the sensor response increased from 16.125 to 0.430 kPa^{-1}, as shown in Fig. 7b, realizing the ultra-sensitive piezoelectric response of all-organic P(VDF-TrFE) nanofibers. In addition, P(VDF-TrFE) could achieve inherent β-phase crystallization and high piezoelectric properties through a low-temperature quenching process, which has huge energy collection potential. Yu[150] employed P(VDF-TrFE) as the matrix, PANI as the conductive filler, and sodium carboxymethyl cellulose (SCMC) as the thickener to prepare a composite aerogel *via* the freeze-drying method. After thermal treatment, β-phase crystals grew during temperature quenching by liquid nitrogen. As shown in Fig. 7c, the freely moving electrons in PANI (Fig. 7d) could promote charge movement in the material through the conductive network formed between PANI and P(VDF-TrFE). The PTNG prepared using PANI/P (VDF-TrFE) exhibited a maximum output voltage of 246 V and short-circuit current of 122 μA, as shown in Fig. 7e, which could light up 119 blue LEDs in series with a size of 3 mm (Fig. 7f). These results lay the foundation for future research and open up new application prospects.

4.1.3 P(VDF-HFP) piezoelectric composites. Although the copolymerization of PVDF with hexafluoropropylene (HFP) decreases its tensile modulus from 2200–2600 MPa to 360–440 MPa, it increases the piezoelectric strain constant and electromechanical coupling coefficient. Similarly, P(VDF-HFP) can be blended with piezoelectric fillers to prepare flexible piezoelectric devices. Zhang *et al.*[142] prepared a PVDF-HFP fiber

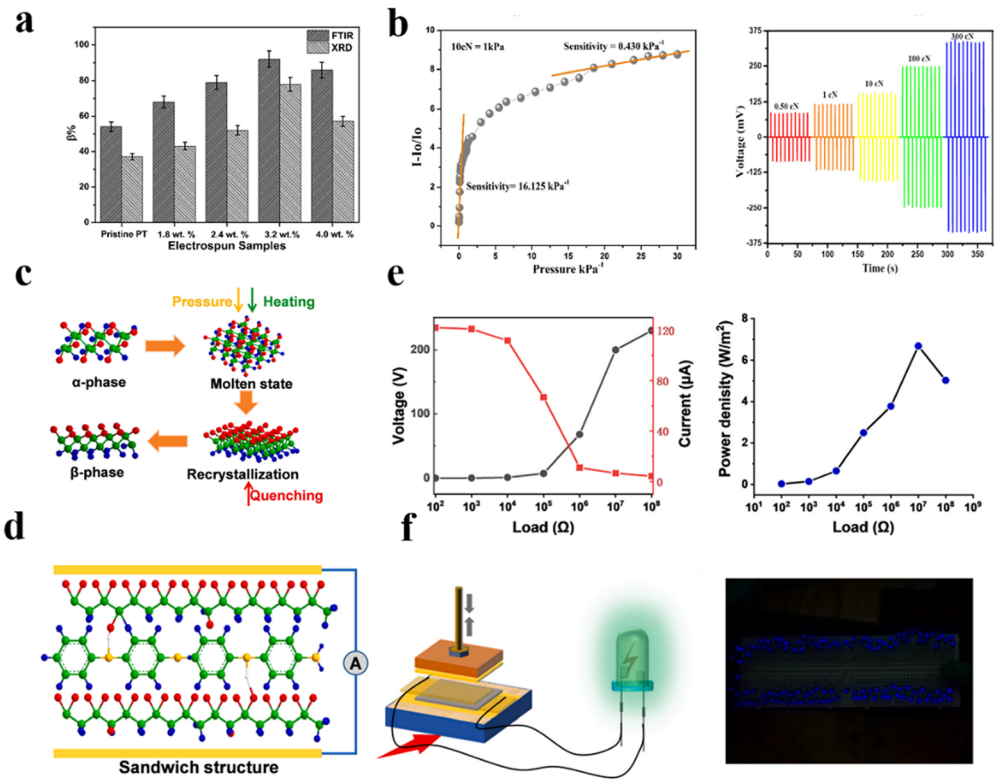

Fig. 7 (a) β-phase content of e-spun nanofibrous mat. (b) Sensitivity of the nanocomposite as a sensor under pressure (left) and a voltage (mV) signal of the pressure sensor with varying pressure (right). Reproduced with permission from ref. 149. Copyright 2022, Springer. (c) Schematic of the phase transformation process of PVDF-TrFE. (d) Conductive network between PANI and PVDF-TrFE through hydrogen bonds and dipole interactions. (e) Voltage and current density of the PTNG with different resistances. (f) Load power density with different resistances and connection diagram of PANI/PVDF-TrFE PTNG (left) and 119 LED bulbs (right). Reproduced with permission from ref. 150. Copyright 2021, Elsevier.

film by electrostatic spinning, and then grew ZnO nanosheets *in situ* on the PVDF-HFP fiber film *via* the hydrothermal method. The content of the polar β phase in the P(VDF-HFP)/ZnO composite fiber film was 79%, the optimum piezoelectric sensing sensitivity based on this film was 1.9 V kPa^{-1}, and a short response time of 20 ms was achieved for forces in the range of 0.02 to 0.5 N with excellent durability and stability for up to 5000 cycles. In addition, P(VDF-HFP) has great potential for the preparation of triboelectric and piezoelectric hybrid nanogenerators (TPENG). Recently, Lee[66] used electrostatic spinning to prepare PVDF-HFP/$Cs_3Bi_2Br_9$/SEBS nanocomposite fibers (LPPS-NFC) (Fig. 8a) as a promising material for energy collectors. The hybrid fibers not only had good stretchability of over 500% (Fig. 8b) and good recoverability (Fig. 8c), but also has excellent electrical output (400 V, 1.63 μA cm^{-2}, and 2.34 W m^{-2}) (Fig. 8d). As a power source for LEDs (Fig. 8e), they could maintain a steady power output for up to five months, indicating their great potential as smart textiles and wearable power sources.

Microstructural construction on P(VDF-HFP) could further improve the performances of the device. For example, Lu *et al.*[151] prepared a PVDF-HFP sponge porous structure membrane *via* solvent-induced phase separation using polyethylene glycol (PEG) as the pore-forming agent and Fe_3O_4@KH550 as the filler. The device based on this PVDF-HFP nanocomposite membrane exhibited a superior piezoelectric coefficient d_{33} of 48.6 pC N^{-1}, sensitivity of 294 mV N^{-1}, power density of 5.3 μW cm^{-3}, and power generation performance of more than 10 000 cycles. The prepared nanogenerator is expected to develop multifunctional responses, high-performance flexible collectors and smart sensors.

4.1.4 Other polymers for piezoelectric composites. Besides PVDF and its copolymers, several types of polymers such as PVC, epoxy resin, PU, and PDMS have also been used to prepare piezoelectric composites. Among them, PDMS-based flexible piezoelectric composites have become a research hotspot in recent years. Zheng *et al.*[152] uniformly dispersed $(Ba_{0.85}Ca_{0.15})(Ti_{0.90}Zr_{0.10})O_3$ (BCZT) nanoparticles in PDMS with the aid of the orientation field of dielectric electrophoresis, which resulted in an open circuit voltage of 29.9 V, excellent sensitivity and extraordinary cyclic stability over a wide pressure range. In another example, Nam *et al.*[153] dispersed boron nitride nanotubes (BNNTs) uniformly in the PDMS matrix *via* a cosolvent method after long and slow agitation and demonstrated the preparation of multifunctional, PDMS/BNNT stretchable piezoelectric composites. The tensile strain of the composites could reach 60%, and in addition, their Young's modulus and thermal conductivity increased by 200% and 120% at 9 wt% BNNT, respectively, and the d_{33} was up to 18 pm V^{-1}.

4.2 Conductive polymers and polymeric composites

Conductive polymers include intrinsic polymers and complex types. The intrinsic conducting polymers can be further divided

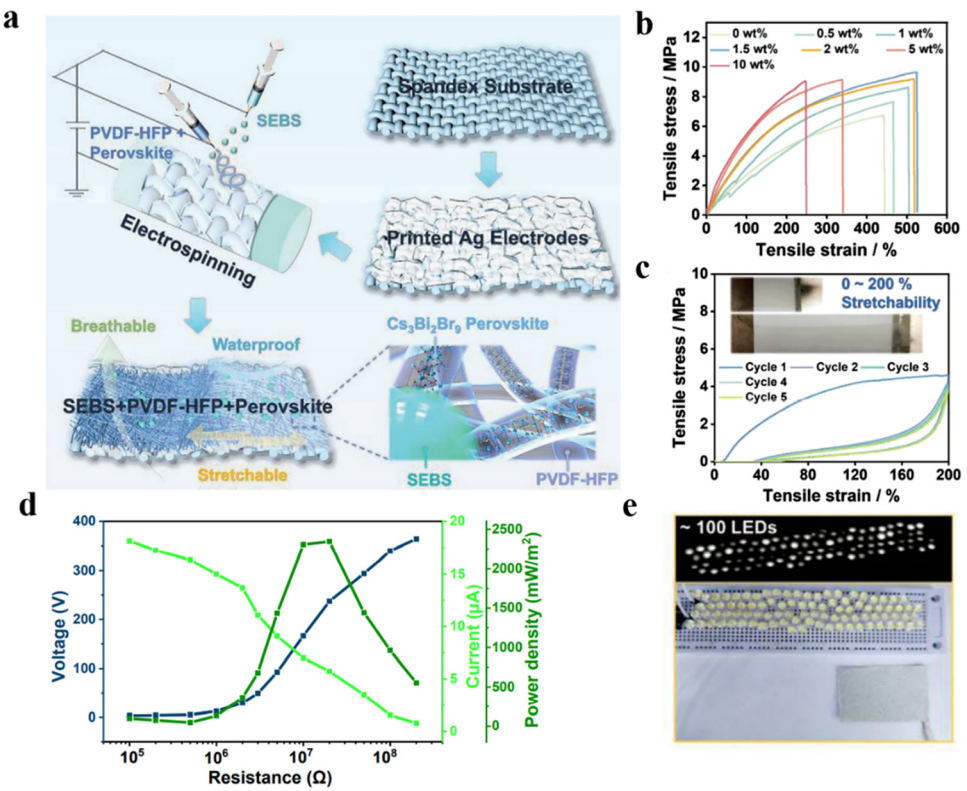

Fig. 8 (a) Schematic demonstration of LPPS-NFC for energy harvesting. (b) Tensile stress–strain curves of the LPPS-NFC. (c) Cyclic tensile stress–strain curves. (d) Voltage, current and power density output of LPPS-NFC-based device. (e) LPPS-NFC-based TPENG drove ≈100 LEDs by tapping. Reproduced with permission from ref. 66. Copyright 2022, Wiley-VCH.

into polymeric semiconductors and polymeric conductors based on their conductivity. In the case of P-type polymer semiconductors such as polythiophene (PT), polysilane and pyrrolopyrrolidone (DPP), holes (positive charges) are mainly used as carriers to realize charge transfer between molecules. Alternatively, N-type polymer semiconductors use electrons (negative charges) as carriers to realize charge transfer, and the classical N-type polymers mainly include imide polymers. A polymeric conductor refers to a polymer that can provide carrier or have electrical conductivity after doping. PANI, polypyrrole (PPy), PT and their derivatives (such as PEDOT)[154–156] based on the unique π–π conjugate structure are attracting wide interest.

Conductive polymeric composites are prepared through various processing technologies (such as solution, melting mix, *in situ* polymerization, spray, spin coating and dip coating), which combines the flexibility of the polymer matrix and functionality of conductive fillers. PDMS, TPU and SBS are frequently used as the polymeric matrix,[88,136,157] while the conductive fillers mainly consist of carbon-based materials (graphite, graphene, CNTs, *etc.*), metal conductors (silver nanowires/nanoparticles, gold nanosheets and copper nanowires) and conductive polymers (PANI, PPy, and PEDOT: PSS).[6,138,158–160] However, although conductive composites have been used for several decades, interestingly there is no generally accepted conclusion about their conductive mechanism to date. Usually, the conducting mechanism is divided into two types, *i.e.*, the tunnel effect and Ohmic conductive law.[161] The tunneling effect theory applies quantum mechanics to understand the relationship between the resistivity of materials and the gap of conductive particles. When the content of conductive fillers is low, most of the conductive fillers separately disperse in the resin matrix and cannot form a conductive pathway. When they are isolated by a thin layer of resin, the adjacent conductive fillers will form an energy barrier after an electrical field is applied. Due to the tunneling effect, electrons can undergo a barrier transition and form a current pathway, as shown in Fig. 9. When the concentration of filler is high, the Ohmic conductive law[12] will play the major role and conductive paths are formed (Fig. 9).

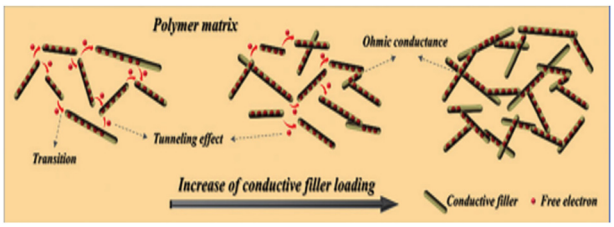

Fig. 9 Schematic illustration of the conductive mechanism of polymer conductive composites. Reproduced with permission from ref. 161. Copyright 2018, The Royal Society of Chemistry.

4.2.1 Poly(3-hexylthiophene) (P3HT). The main chain of P3HT contains a coplanar π-conjugated structure, and there is also π–π interactions between its molecular chains, which contribute to the formation of a supramolecular packing structure and promote the intramolecular and intermolecular charge from the domain. The P3HT molecular chains can be packed to form a crystal and it can have high crystallinity. It is considered as one of the most useful polymeric semiconductors due to its unique photoelectric properties, feasible commercialization, simple synthesis and low costs. Currently, it is used as the active layer material for flexible solar cells, flexible complementary circuits and OLEDs.

When P3HT is used as the active layer in flexible solar cells, its wide bandgap (~1.9 eV) and absorption cut-off wavelength at 650 nm limit the overall efficiency. Thus, various acceptors have been designed to improve the photovoltaic performance of P3HT. For example, Sarah Holliday *et al.*[162] presented a new non-fullerene acceptor that was specifically designed to improve the performance together with the wide bandgap of the donor P3HT, and the efficiency of device reached 6.4%, which was the highest value reported for a fullerene-free P3HT. Secondly, the P-type semiconductor P3HT can be used as the active layer of the OTFT by using holes as carriers under the combined action of the gate source voltage and drain–source voltage. P3HT films are usually deposited *via* the central spin coating method.[163] Unfortunately, the resulting orientation of the π-conjugated plane usually shows a mixed state along the vertical and parallel directions, resulting in low crystallinity and current carrier transmission.[164] To improve the carrier mobility of the P3HT film in the complementary circuit, Lee *et al.* fabricated an organic/inorganic hybrid complementary inverter operating at low voltage (1 V or less) by transferring pressed P-type P3HT and inorganic N-type ZnO electrolytic transistors (EGT). The device performance (transfer curves, carrier mobility, on–on voltage, and on/off ratio) clearly demonstrated the excellent reliability of the stamping method for implementing electronic circuits. Lastly, P3HT has been used as a hole injection layer (HIL) of OLEDs to significantly improve their performance.[165] Recently, Kim and co-workers[166] fabricated an OLED by spinning tris(pentafluorophenyl) borane (BCF)-doped P3HT (P3HT: BCF) nanolayers on ITO electrodes, and then depositing organic layers and top electrodes. The luminance increased dramatically to 26 910 cd m^{-2}, resulting in a high current efficiency of about 19 cd A^{-1}. They demonstrated that the P3HT: BCF hole injection layer was successfully applied in a flexible OLED.

4.2.2 PEDOT:PSS. PEDOT is a hydrophobic conjugated polymer whose hydrophilic PSS can disperse PEDOT in an aqueous solution. The conductivity of PEDOT:PSS films is highly dependent on the ratio of PEDOT to PSS and the particle size of PEDOT:PSS dispersed in water. Once the PEDOT: PSS film is formed, its conductivity will be limited by the content of PSS, which is usually less than 10 S cm^{-1},[167] and the conductivity and carrier mobility are much lower than that of the traditional inorganic conductors. The conductivity of PEDOT: PSS films can usually be improved by introducing additives or by post-treatment with various solutions. Common additives include acids (sulfuric acid, methanesulfonic acid, *etc.*),[63,168] polar solvents (dimethyl sulfoxide, ethylene glycol, diethylene glycol, *etc.*),[169,170] and surfactants.[171] For example, Fan *et al.*[63]

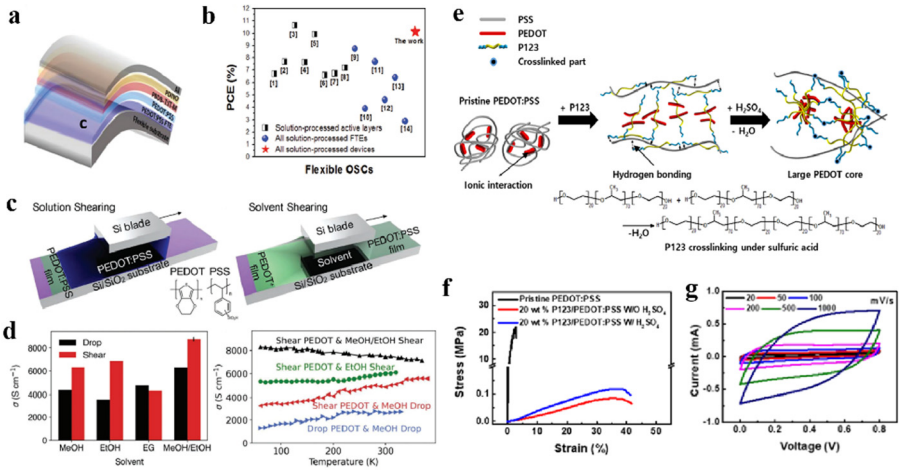

Fig. 10 (a) Schematic architecture of all-solution-processed flexible OSCs. (b) Plotted values of PCEs of flexible OSCs reported recently. Reproduced with permission from ref. 63. Copyright 2018, Wiley-VCH. (c) Schematic of sheared deposition of PEDOT: PSS. (d) Typical conductivities of sheared PEDOT: PSS films with post-deposition treatments with different solvents. (d) Temperature dependence of the conductivity of individual deposited PEDOT: PSS films. Reproduced with permission from ref. 173. Copyright 2021, Wiley-VCH. (e) Schematic of the possible scenario in the modification of PEDOT: PSS. (f) Stress–strain curves of free-standing pristine PEDOT: PSS. (g) CV curves of the supercapacitor with a variation in scan rate. Reproduced with permission from ref. 62. Copyright 2018, the American Chemistry Society.

treated PEDOT: PSS with methanesulfonic acid (CH_4SO_3) at room temperature ($\approx$20 °C) and formed a smooth and uniform PEDOT: PSS film with high optical and electrical properties. Subsequently, full-solution OSCs with a PEDOT: PSS electrode were prepared (Fig. 10a). The maximum power conversion efficiency of the flexible OSC devices prepared using this PEDOT: PSS film was 10.12% (Fig. 10b). In addition, the conductivity of the PEDOT: PSS film increased to about 5000 S cm^{-1} by post-treatment of the film with concentrated sulfuric acid.[172] The selection of appropriate processing methods can also significantly improve the conductivity of PEDOT: PSS films. Recently, Bao *et al.*[173] reported a solvent shearing technique to improve the arrangement and relative percentage of conductive PEDOT phases in PEDOT: PSS films (Fig. 10c). This shear deposition and solvent treatment can be easily integrated into a high-throughput roll-coating process. After shearing, the thin film presented an anisotropic arrangement of PEDOT-rich phase in the shear direction, resulting in a breakthrough room temperature conductivity of 8500 $\pm$ 400 S cm^{-1} (Fig. 10d).

However, an obvious disadvantage of the original PEDOT: PSS film is its low stretchability (<6%).[174] It is difficult to maintain both high conductivity and stretchability, and its resistance can be seriously affected by strain. It has been reported that the conductivity of stretchable PEDOT: PSS films can be increased to 2890 S cm^{-1} using methanesulfonic acid post-treatment, but the resistance increased by 30 times under 30% tensile strain.[164] Lee *et al.*[62] modified PEDOT: PSS using the poly(ethylene glycol)-*B*-poly(propylene glycol)-*B*-poly(ethylene glycol) triblock copolymer (Fig. 10e), and then used sulfuric acid for post-treatment to prepare a transparent PEDOT: PSS film. The resulting blend showed conductivity of 1700 S cm^{-1} and good tensile properties (Fig. 10f). The resistance only changed by 4% after 1000 cycles of stretching (Fig. 10g), indicating that the resistance is hardly affected by the deformation. However, there is no intrinsic conductive polymer with high ductility that can be used as a flexible electrode. Thus, the low tensile limit and high manufacturing cost are problems that need to be further solved, and the choice of the composite conductive polymer may be a better choice to realize flexible active elements.

4.2.3 PDMS conductive composites. PDMS conductive composites have a wide range of potential applications in fields such as human–computer interaction, electronic skins, personal health care and motion performance monitoring. They are also pressure-sensitive materials (PSR) for the preparation of piezoresistive sensors and can be easily attached to curved surfaces such as the human body and deformable surgical tools. However, to meet practical needs, PDMS is integrated with conductive composites with important properties such as self-healing ability[175] and superhydrophobicity.[176,177]

Given that PDMS elastomers are chemically crosslinked, their conductive composites are usually prepared *via* a simple solution pouring molding method. For example, Fu *et al.*[161] prepared silanized cellulose nanocrystals (SCNC)/CNT nanocrystals *via* the solution casting method. The SCNC-CNT/PDMS-assembled strain sensor showed a high strain range of more than 100% and had good strain sensitivity, with a gauge factor (GF) of 37.11 at 50 °C, providing long-term stability and durability. To achieve high sensitivity and flexibility, researchers have adopted some special preparation methods to prepare PDMS conductive composites to obtain better comprehensive performances. Hu *et al.*[178] let carbon black nanoparticles (nCB) diffuse in PDMS to form a gradient distribution, as illustrated in Fig. 11a. The mechanical properties of the PDMS/nCB composites obtained were observed to be close to that of pure PDMS, with elongation at break, tensile strength and modulus of 361%, 0.483 MPa and 0.55 MPa, respectively (Fig. 11b). When

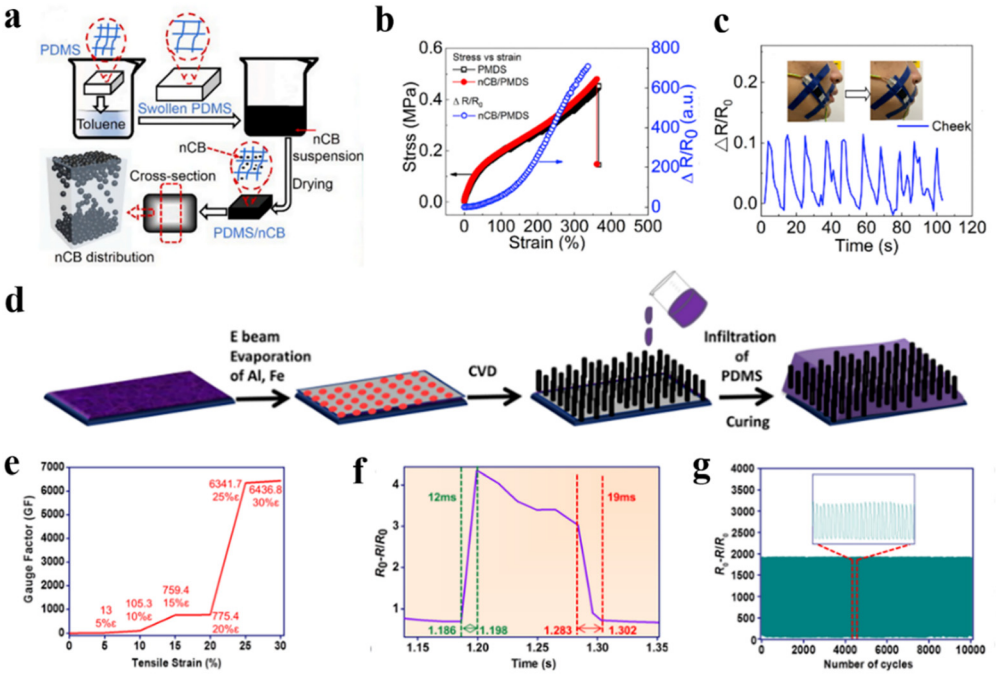

Fig. 11 (a) Schematic of the procedure for the preparation of PDMS/nCB nanocomposites. (b) Stress and relative resistance change *versus* strain. (c) Cycled electromechanical behaviors of PDMS/nCB at different speeds of air blowing on the cheek. Reproduced with permission from ref. 178. Copyright 2020, Elsevier. (d) Schematic diagram of the fabrication process of the VACNT/PDMS thin-film. (e) GF as a function of stretchability. (f) Dynamic response time of the VACNT/PDMS thin-film sensor. (g) Electromechanical stability of the VACNT/PDMS thin film for 10 000 sequential tensile cycles. Reproduced with permission from ref. 179. Copyright 2021, the American Chemistry Society.

the nCB content was 6.2 wt%, the GF reached 343 and the strain reached 355%, which could be used as a high-performance flexible strain sensor to detect the finger or facial movements (Fig. 11c). Elizabeth *et al.*[179] manufactured a vertically aligned carbon nanotube (VACNT)/PDMS thin film, and the preparation process is shown in Fig. 11d. A CNT thin film was obtained on an SiO_2/Si substrate *via* the chemical vapor deposition (CVD) method and the PDMS seamlessly permeated in the adjacent VACNT gap. The final device showed attractive properties, with the detectable strain in the range of 0.004% to 30%, GF of 6436.8 (Fig. 11e) under 30% strain, ultra-fast response time of 12 ms, recovery time of 19 ms (Fig. 11f) and excellent reproducibility in 10 000 cycles (Fig. 11g).

4.2.4 TPU conductive composites. Compared with chemically crosslinked PDMS, TPU can be compounded with conductive materials through a variety of processing techniques. Kumar *et al.*[180] prepared MWCNT/TPU nanocomposites *via* solution mixing combined with high-speed homogenization process, as shown in SEM (Fig. 12a). MWCNT/TPU strain sensors can achieve adjustable strength, sensitivity and strain tolerance. Taking 0.3 wt% MWCNT load as an example, the GF was 22 when the strain was below 15%, which increased to 6395 at 35% strain and 6423 at 95% strain. Although the detection limit has been expanded, it is still a challenge to achieve high tensile and sensitivity simultaneously, and the response stability and durability still need to be improved.[181] Shao *et al.*[182] prepared a TPU fiber membrane *via* electrostatic spinning and prepared polyaniline nanoparticles (PANIP) on the TPU fiber

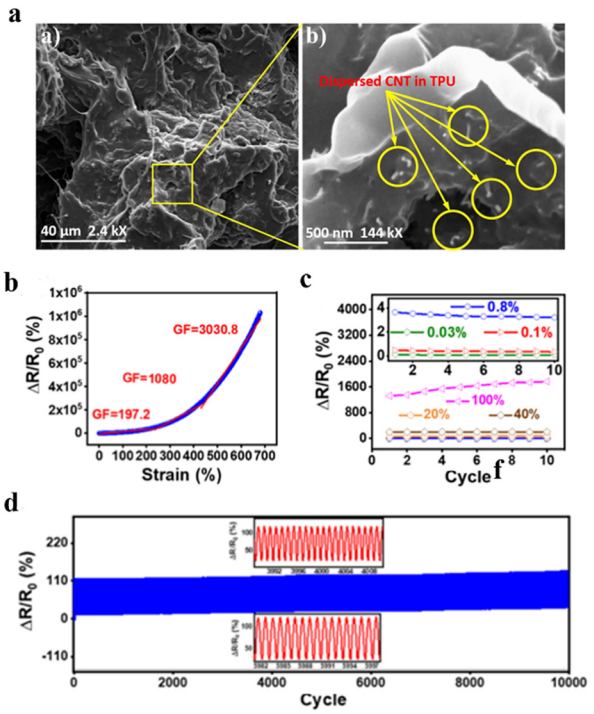

Fig. 12 (a) SEM images of TPUEM/CNTs/AgNPs. Reproduced with permission from ref. 180. Copyright 2019, Wiley-VCH. (b) $\Delta R/R_0$ of CPUF vs strain. (c) Maximum values of CPUF at the strain of 0.03% to 100%. (d) Long-term stability during 10 000 cycles. Reproduced with permission from ref. 182. Copyright 2022, the American Chemistry Society.

membrane *via in situ* polymerization. Fig. 12b shows that small strain could cause weak damage on the conductive network and led to a small increase in resistance. When the strain further increased, large-size cracks appeared and the PANIP and CB particles started to separate, and consequently the GF increased to 1080. This interesting structure endowed the TPU strain sensor with an attractive performance including maximum strain of up to 680%, GF of up to 3030.8, high sensitivity of 0.03% strain (Fig. 12c) and excellent durability for at least 10 000 stretch/release cycles (Fig. 12d).

4.2.5 SBS conductive composites. SBS is a typical thermoplastic elastomer, in which its styrene segments aggregate to form physical crosslinking points and the butadiene phase is the elastic matrix. Because of the π–π interaction between its phenyl groups and carbon atoms, SBS has good miscibility with carbon conductive fillers.[9] Compared with PDMS and TPU, SBS has an interesting advantage, where it can carry high concentration of metal nanofillers, which can maximize the conductivity of nanocomposites.[183] Hyeon *et al.*[137] reported the preparation of a soft Ag–Au/SBS nanocomposite with high conductivity and biocompatibility *via* a solvent-induced phase separation method. Owing to the high aspect ratio and percolation network of the Ag–Au nanowires, the nanocomposites exhibited an optimized conductivity of 41 850 S cm^{-1} (Fig. 13a) and yielded an optimized stretchability of 266% (maximum of 840%) (Fig. 13b). They successfully prepared wearable (Fig. 13c) and implantable electrodes (Fig. 13d) for biosensing and stimulation of human skin and pig heart, respectively. Alternatively, coating, printing and even spinning techniques can be applied to SBS solution. Chen *et al.*[172] prepared SBS/MWCNT cored sheath fibers (SSCCSF) *via* the coaxial wet spinning method. SEM (Fig. 13e) showed that SSCCSF has a bean-shaped cross-section with SBS as the core and SBS/MWCNTs as the sheath. The SSCCSF sensor exhibited a high sensitivity of 25 832.77 at 41.5% strain, which was capable of detecting large movements in the human body (Fig. 13f) and subtle physiological activities (Fig. 13g). Nevertheless, similar to TPU, the residual strain after large deformation is a significant disadvantage of the SBS conductive composite. Alternatively, the adhesion of SBS has also been utilized. Jeong *et al.*[184] found that the SBS/Au composite could adhere to a chemically crosslinked substrate with good conformability.

4.3 Polymeric dielectric composites

Polymeric elastomers usually have a low dielectric constant (<10), and the study on polymeric dielectrics with high dielectric constant, low dielectric loss and good flexibility are of great significance.[93,185] Similar to the common preparation of composites, dielectric composites are prepared by blending inorganic particles or conductive particles with elastomers.[185–187] Currently, the most widely used elastomers are PDMS and TPU, with high dielectric fillers including ferroelectric ceramic fillers such as BTO,[124] barium strontium titanate (BST),[188] and titanium dioxide (TiO_2)[189] and conductive fillers including metal nanoparticles and carbon nanomaterials.[134,187,190]

PDMS is the most frequently used dielectric elastomer material for the fabrication of flexible devices due to its

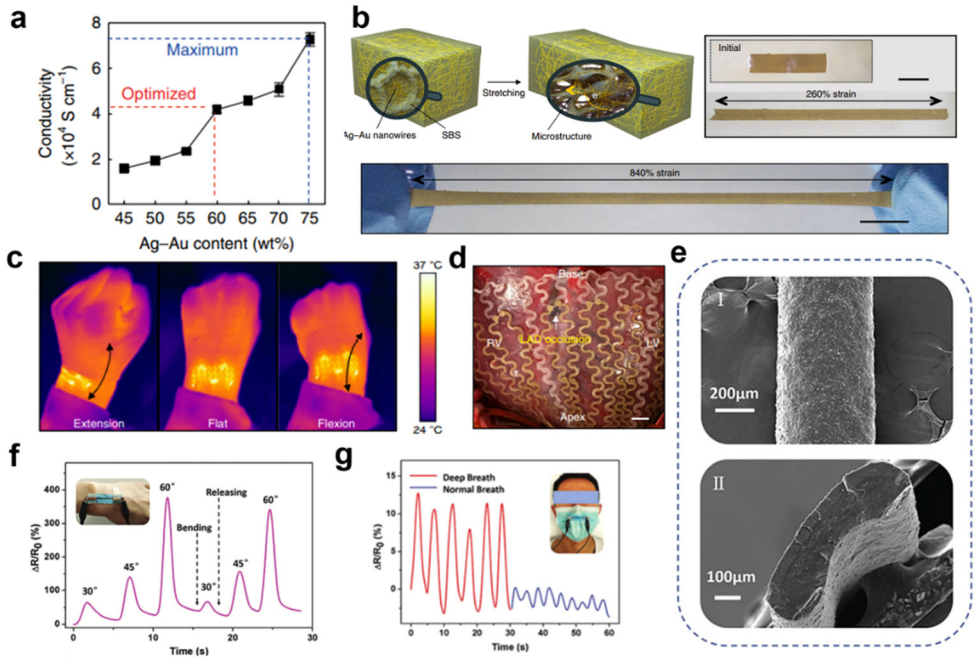

Fig. 13 (a)Schematic illustration of the microstructured Ag–Au nanocomposite before and after stretching. (b) Optical image of the Ag–Au nanocomposite. (c) Infrared camera images showing reliable heating performance of the wearable device on a wrist. (d) Optical camera image of implanted cardiac mesh on a swine heart. Reproduced with permission from ref. 137. Copyright 2018, the Author(s). (e) SEM of SBS/MWCNTs core-sheath fiber. (f) Interphalangeal joint bending test. (g) Breathing test. Reproduced with permission from ref. 172. Copyright 2020, Wiley-VCH.

excellent elastic properties and biomedical compatibility. For example, Fu *et al.*[190] prepared a flexible capacitive tactile sensor, employing a CNT/PDMS composite film as the dielectric layer, and deposited gold on PI film as the electrode. The sensitivity reached 1.61% kPa^{-1} at pressures below 1 MPa. The prepared tactile sensor exhibited an ultra-wide pressure operating range of 0.9 kPa–2.55 MPa and excellent stability and fast response time. Alternatively, PDMS can capture negative charge and be decorated with various microstructures, making it a candidate material for the friction layer of triboelectric nanogenerators. Wang *et al.*[30] filled the PDMS matrix with silver nanoparticles and embedded microcapacitors (MCs) and variable microcapacitors (VMCs) in PDMS. Then, a TENG was prepared based on the VMC@PDMS film, which effectively improved the output current. Under 20 m resistance load, the output power density was up to 6 W m^{-2}. This unit could be used to illuminate about 100 green LED in series and exhibited good stability after thousands of cycles.

TPU has also been frequently used. Wang *et al.*[191] incorporated AgNW as a dielectric filler in a TPU nanofiber membrane to construct a composite dielectric layer. The micro-network structure of TPU and AgNW had a synergistic effect and the sensitivity of the capacitive pressure sensor reached 7.24 kPa^{-1} in the low-pressure range (9.0×10^{-3} to 0.98 kPa). TPU foams have also been adopted due to their high porosity, good mechanical flexibility and low compression modulus. Park *et al.*[192] used perovskite derivative oxide (CCTO) to wrap PU sponge with low modulus. The porous PU scaffold reduced the compression modulus and the dielectric constant of the composite was significantly improved. They produced a highly sensitive, stretchable and flexible capacitive sensor with sensitivity of 0.73 kPa^{-1} ($<$1.6 kPa), response time of 84 ms, and stability over 7600 cycles.

5 Conclusions and outlook

This review was prepared at a time in which flexible electronics are the focus of both academic research and industry. The purpose of this work is to illustrate the useful polymers for the fabrication of these devices, and, more importantly, to illuminate the features of key materials that are needed for future flexible electronics, which can continuously support their own activities. Based on this consideration, we divided flexible electronics into three parts, including self-sustainable energy power devices, displays and sensors (interaction). Employing these three components, flexible devices can collect data and communicate information. The polymers used in these components can be basically classified into two types based on their functionality, including non-functional polymers (substrates and adhesives) and functional polymeric composites.

In the case of non-functional polymers, they are mostly used as substrates and adhesives. Although most polymeric matrices can be feasibly manufactured by traditional techniques, which significantly reduce the cost, their major disadvantages include low heat-resistance capability and anti-fatigue behaviour. Other specific challenges include transparency, gas barrier property, self-healing and biodegradability. One of the most effective ways to meet one or several demands is the molecular design of polymer chains and condensed structures. Nevertheless, this may not be the most economical way. Alternatively, polymeric adhesives have versatile molecular architectures in both industry and academia.

In the case of functional polymeric composites, which act as the key components of power supply, sensor, *etc.*, they can be mostly prepared by solution or melt blending. Not only the species of fillers and polymers can be optimized, but also the processing technique is crucial in increasing the capability of these key materials. Crystallization, microphase separation, dispersion of fillers, and the construction of gradual or pore structures can all be controlled to optimize the overall behaviour of the final device. Together with the above-mentioned limitations originating from the nature of functional polymeric composites.

Among the above-discussed polymers, obviously, PDMS, TPU, PI, PVDF and their derivatives and composites are very important candidates for the preparation of flexible electronics. Nevertheless, in the future, specific polymers with modified or customized properties toward specific applications should be developed. This is because the mechanical properties, sensor range, sensitivity, sustainable power supply, *etc.* always require better behaviours. Nevertheless, we have sufficient reason to believe that toward long-term flexible electronics, polymers can always find value and irreplaceable roles.

In the case of polymeric substrates, plastic substrates have the disadvantages of low processing temperature, insufficient sealing, poor thermal stability, deformation, *etc.*, and elastomer substrates need further improvement of their fatigue resistance and interface adhesion with functional elements. Their properties should be improved by re-designing the molecular chain structure and microstructure of polymer substrates. Another effective method is to explore new polymers with excellent comprehensive performances to meet higher requirements. In addition, as the requirements of flexible electronics gradually increase, biodegradable substrates, stimuli-responsive substrates, self-healing substrates, and substrates with shape-memory functions have been reported widely, and substrates integrated into multifunctional devices or used in extreme environments also need to be further studied. In the case of polymer adhesive materials, such as mussels-inspired hydrogel adhesives, they have excellent adhesion properties, biocompatibility and self-healing performances, but they are limited to soft systems. Therefore, it is urgent to invest more efforts to extending the current scope to high-hardness and dry systems, such as elastomer adhesives. In addition, novel adhesion enhancement mechanisms and strategies need to be explored to solve the mechanical mismatch problem caused by the different thermal expansion coefficients of different adhesives.

Polymeric composites as functional materials are used in flexible electronic devices including piezoelectric composites, conductive composites and dielectric composites. Firstly, the ferroelectric fatigue of piezoelectric composites is a problem

that cannot ignored, and the mechanism of fatigue is not clear at present. Future work should focus on intelligent electronics and biocompatible devices and research on PVDF-based polymer devices may shift attention from basic functions to complex applications. Due to the biocompatibility of PVDF-based polymers, more and more researchers will use them in implantable devices and artificial prosthetics. Secondly, in the case of conductive composites, it is well known that effective conductive networks need a high filler content, which will further reduce the flexibility of the elastic matrix, and thus it is necessary to carry out modifications to optimize the compatibility between the filler and matrix. Alternatively, it is essential to explore new conductive composites through the optimization of molecular design and novel preparation technology to modulate the micro and macro structures. Recently, researchers have started to explore conductive composites by 3D printing, selective laser sintering, two-photon polymerization printing and other new technologies. In addition, it is worth noting that some polymeric semiconductors, such as poly(*p*-phenylene vinyl) (PPV), poly(furan) (PF) and PT composites have not been explored to date, and it is expected that the development of these materials will yield great application prospects. Lastly, dielectric composites require a high amount of ceramic fillers for improving their dielectric constant, but this is at the cost of mechanical properties. Besides, the dielectric constant is significantly increased at a lower amount of conductive fillers, resulting in high dielectric loss. Therefore, it is necessary to reasonably design the microstructure of composite materials to achieve a reasonable balance of properties and actively explore and develop new dielectric materials and conductive fillers to meet the new demands for flexible electronic products.

Conflicts of interest

There are no conflicts to declare.

Acknowledgements

This work was financially supported by The Key Research and Development Program of Zhejiang Province (2019C03074), Ningbo Technological Innovation of 2025 (2020Z086, 2021Z070, 2022Z150), Zhejiang Health Technology Program (2022514106), Ningbo Public Benefit Project (2022S136).

References

1 A. Bouhamed, Q. Binyu, B. Böhm, N. Jöhrmann, N. Behme, W. A. Goedel, B. Wunderle, O. Hellwig and O. Kanoun, *Compos. Sci. Technol.*, 2021, **208**, 108769.
2 X. Cao, Y. Xiong, J. Sun, X. Zhu, Q. Sun and Z. L. Wang, *Adv. Funct. Mater.*, 2021, **31**, 2102983.
3 D. Koo, S. Jung, J. Seo, G. Jeong, Y. Choi, J. Lee, S. M. Lee, Y. Cho, M. Jeong, J. Lee, J. Oh, C. Yang and H. Park, *Joule*, 2020, **4**, 1021–1034.
4 Y. Xue, L. Wang, Y. Zhang, G. Liang, J. Chu, B. Han, W. Cao, C. Liao and S. Zhang, *IEEE Electron Device Lett.*, 2021, **42**, 188–191.
5 X. Zhao and Z. Ounaies, *Nano Energy*, 2022, **94**, 106908.
6 S. Zheng, Y. Jiang, X. Wu, Z. Xu, Z. Liu, W. Yang and M. Yang, *Compos. Sci. Technol.*, 2021, **201**, 108546.
7 F. De Rossi, G. Renno, B. Taheri, N. Yaghoobi Nia, V. Ilieva, A. Fin, A. Di Carlo, M. Bonomo, C. Barolo and F. Brunetti, *J. Power Sources*, 2021, **494**, 229735.
8 K. Sim, Z. Rao, F. Ershad and C. Yu, *Adv. Mater.*, 2020, **32**, e1902417.
9 I. You, M. Kong and U. Jeong, *Acc. Chem. Res.*, 2019, **52**, 63–72.
10 W. Kong, Y. Yang, Y. Wang, H. Cheng, P. Yan, L. Huang, J. Ning, F. Zeng, X. Cai and M. Wang, *J. Mater. Chem. A*, 2022, **10**, 2012–2020.
11 S. Li, Y. Cong and J. Fu, *J. Mater. Chem. B*, 2021, **9**, 4423–4443.
12 H. Liu, Q. Li, S. Zhang, R. Yin, X. Liu, Y. He, K. Dai, C. Shan, J. Guo, C. Liu, C. Shen, X. Wang, N. Wang, Z. Wang, R. Wei and Z. Guo, *J. Mater. Chem. C*, 2018, **6**, 12121–12141.
13 X. Xu, K. Fukuda, A. Karki, S. Park, H. Kimura, H. Jinno, N. Watanabe, S. Yamamoto, S. Shimomura, D. Kitazawa, T. Yokota, S. Umezu, T. Q. Nguyen and T. Someya, *Proc. Natl. Acad. Sci. U. S. A.*, 2018, **115**, 4589–4594.
14 F. R. Fan, Z. Q. Tian and Z. Lin Wang, *Nano Energy*, 2012, **1**, 328–334.
15 S. D. Mahapatra, P. C. Mohapatra, A. I. Aria, G. Christie, Y. K. Mishra, S. Hofmann and V. K. Thakur, *Adv. Sci.*, 2021, **8**, e2100864.
16 Z. L. W. J. H. Song, *Science*, 2006, **312**, 242–246.
17 R. Sahoo, S. Mishra, A. Ramadoss, S. Mohanty, S. Mahapatra and S. K. Nayak, *Polymer*, 2020, **205**, 122869.
18 X. Liang, T. Zhao, W. Jiang, X. Yu, Y. Hu, P. Zhu, H. Zheng, R. Sun and C.-P. Wong, *Nano Energy*, 2019, **59**, 508–516.
19 S. Sinha, R. Daniels, O. Yassin, M. Baczkowski, M. Tefferi, A. Deshmukh, Y. Cao and G. Sotzing, *Adv. Mater. Technol.*, 2021, **7**, 2100548.
20 H. Kim, J. Park, T. Khim, S. Bak, J. Song and B. Choi, *Sci. Rep.*, 2021, **11**, 8387.
21 H. Wang, X. Yang, S. Zhang, Z. Liu, L. Liu, B. Cai, S. Shi and D. Wang, *Chin. J. Liq. Cryst. Disp.*, 2022, **37**, 451–458.
22 Z. H. Yang, C. Q. Kang, H. Q. Guo and L. X. Gao, *Acta Polym. Sin.*, 2021, **52**, 1308–1315.
23 L. Beker, N. Matsuhisa, I. You, S. R. A. Ruth, S. Niu, A. Foudeh, J. B. Tok, X. Chen and Z. Bao, *Proc. Natl. Acad. Sci. U. S. A.*, 2020, **117**, 11314–11320.
24 J. Kang, D. Son, G. N. Wang, Y. Liu, J. Lopez, Y. Kim, J. Y. Oh, T. Katsumata, J. Mun, Y. Lee, L. Jin, J. B. Tok and Z. Bao, *Adv. Mater.*, 2018, **30**, e1706846.
25 Y. Khan and Z. Bao, *Proc. Natl. Acad. Sci. U. S. A.*, 2021, 118.
26 I. You, D. G. Mackanic, N. Matsuhisa, J. Kang, J. Kwon, L. Beker, J. Mun, W. Suh, T. Y. Kim, J. B. H. Tok, Z. N. Bao and U. Jeong, *Science*, 2020, **370**, 961.
27 J. A. Rogers, Z. Bao, A. Dodabalapur and A. Makhija, *IEEE Elctron Devices Lett.*, 2000, **21**, 100–103.

28 H. Klauk, U. Zschieschang, J. Pflaum and M. Halik, *Nature*, 2007, **445**, 745–748.
29 K. Huang, Y. Peng, Y. Gao, J. Shi, H. Li, X. Mo, H. Huang, Y. Gao, L. Ding and J. Yang, *Adv. Energy Mater.*, 2019, **9**, 1901419.
30 Afrasiab, A. D. Khan, F. E. Subhan, A. D. Khan, S. D. Khan, M. S. Ahmad, M. S. Rehan and M. Noman, *Optik*, 2020, **208**, 164573.
31 Q. Dong, Y. Xue, S. Wang, L. Wang, F. Chen, S. Zhang, R. Chi, L. Zhao and Y. Shi, *Sci. China Mater.*, 2017, **60**, 963–976.
32 X. Xia, J. Chen, H. Guo, G. Liu, D. Wei, Y. Xi, X. Wang and C. Hu, *Nano Res.*, 2016, **10**, 320–330.
33 S. Sukumaran, S. Chatbouri, D. Rouxel, E. Tisserand, F. Thiebaud and T. Ben Zineb, *J. Intell. Mater. Syst. Struct.*, 2020, **32**, 746–780.
34 Y. Wang, L. Zhu and C. Du, *Micromachines*, 2021, **12**, 1278.
35 L. Wang, H. Wang, X.-W. Huang, X. Song, M. Hu, L. Tang, H. Xue and J. Gao, *J. Mater. Chem. A*, 2018, **6**, 24523–24533.
36 S. Wang, P. Xiao, Y. Liang, J. Zhang, Y. Huang, S. Wu, S.-W. Kuo and T. Chen, *J. Mater. Chem. C*, 2018, **6**, 5140–5147.
37 Y. Zhao, M. Ren, Y. Shang, J. Li, S. Wang, W. Zhai, G. Zheng, K. Dai, C. Liu and C. Shen, *Compos. Sci. Technol.*, 2020, **200**, 108448.
38 Y. Lin, S. Q. Liu, S. Chen, Y. Wei, X. C. Dong and L. Liu, *J. Mater. Chem. C*, 2016, **4**, 6345–6352.
39 M. Wang, K. Zhang, X. X. Dai, Y. Li, J. Guo, H. Liu, G. H. Li, Y. J. Tan, J. B. Zeng and Z. Guo, *Nanoscale*, 2017, **9**, 11017–11026.
40 J. Shen, Y. Guo, S. Zuo, F. Shi, J. Jiang and J. Chu, *Nanoscale*, 2021, **13**, 19155–19164.
41 F. X. Wang, S. H. Zhang, L. J. Wang, Y. L. Zhang, J. Lin, X. H. Zhang, T. Chen, Y. K. Lai, G. B. Pan and L. N. Sun, *J. Mater. Chem. C*, 2018, **6**, 12575–12583.
42 Z. Jin, L. Yang, S. Shi, T. Wang, G. Duan, X. Liu and Y. Li, *Adv. Funct. Mater.*, 2021, **31**, 2103391.
43 Y. Yang, M. Zhou, J. Peng, X. Wang, Y. Liu, W. Wang and D. Wu, *Carbohydr. Polym.*, 2022, **276**, 118753.
44 L. Travaglini, A. P. Micolich, C. Cazorla, E. Zeglio, A. Lauto and D. Mawad, *Adv. Funct. Mater.*, 2020, **31**, 2007205.
45 Y. Yao, W. Huang, J. Chen, G. Wang, H. Chen, X. Zhuang, Y. Ying, J. Ping, T. J. Marks and A. Facchetti, *Proc. Natl. Acad. Sci. U. S. A.*, 2021, **118**, e2111790118.
46 G. Cantarella, J. Costa, T. Meister, K. Ishida, C. Carta, F. Ellinger, P. Lugli, N. Münzenrieder and L. Petti, *Flexible Printed Electron.*, 2020, **5**, 033001.
47 X. Chen, G. Xu, G. Zeng, H. Gu, H. Chen, H. Xu, H. Yao, Y. Li, J. Hou and Y. Li, *Adv. Mater.*, 2020, **32**, e1908478.
48 J. Kim, D. Ouyang, H. Lu, F. Ye, Y. Guo, N. Zhao and W. C. H. Choy, *Adv. Energy Mater.*, 2020, **10**, 1903919.
49 Y. Wang, Q. Chen, G. Zhang, C. Xiao, Y. Wei and W. Li, *ACS Appl. Mater. Interfaces*, 2022, **14**, 5699–5708.
50 P. Wen, R. Peng, W. Song, J. Ge, X. Yin, X. Chen, C. Liu, X. Zhang and Z. Ge, *Org. Electron.*, 2021, **94**, 106172.
51 S. Kim, H. Oh, I. Jeong, G. Kang and M. Park, *ACS Appl. Electron. Mater.*, 2021, **3**, 3207–3217.
52 J. A. Spechler, T.-W. Koh, J. T. Herb, B. P. Rand and C. B. Arnold, *Adv. Funct. Mater.*, 2015, **25**, 7428–7434.
53 D. Y. Cho, Y. H. Shin and H. K. Kim, *Surf. Coat. Technol.*, 2014, **259**, 109–112.
54 X. Dong, P. Shi, L. Sun, J. Li, F. Qin, S. Xiong, T. Liu, X. Jiang and Y. Zhou, *J. Mater. Chem. A*, 2019, **7**, 1989–1995.
55 S. B. Kang, H. J. Kim, Y. J. Noh, S. I. Na and H. K. Kim, *Nano Energy*, 2015, **11**, 179–188.
56 H. C. Weerasinghe, P. M. Sirimanne, G. P. Simon and Y. B. Cheng, *Prog. Photovoltaics Res. Appl.*, 2012, **20**, 321–332.
57 J. Yoon, H. Sung, G. Lee, W. Cho, N. Ahn, H. S. Jung and M. Choi, *Energy Environ. Sci.*, 2017, **10**, 337–345.
58 I. Jeon, K. Cui, T. Chiba, A. Anisimov, A. G. Nasibulin, E. I. Kauppinen, S. Maruyama and Y. Matsuo, *J. Am. Chem. Soc.*, 2015, **137**, 7982–7985.
59 X. Meng, L. Zhang, Y. Xie, X. Hu, Z. Xing, Z. Huang, C. Liu, L. Tan, W. Zhou, Y. Sun, W. Ma and Y. Chen, *Adv. Mater.*, 2019, **31**, e1903649.
60 D. H. Shin, S. W. Seo, J. M. Kim, H. S. Lee and S. H. Choi, *J. Alloys Compd.*, 2018, **744**, 1–6.
61 H. H. Tang, H. R. Feng, H. K. Wang, X. J. Wang, J. J. Liang and Y. Chen, *ACS Appl. Mater. Interfaces*, 2019, **11**, 25330–25337.
62 J. H. Lee, Y. R. Jeong, G. Lee, S. W. Jin, Y. H. Lee, S. Y. Hong, H. Park, J. W. Kim, S. S. Lee and J. S. Ha, *ACS Appl. Mater. Interfaces*, 2018, **10**, 28027–28035.
63 W. Song, X. Fan, B. Xu, F. Yan, H. Cui, Q. Wei, R. Peng, L. Hong, J. Huang and Z. Ge, *Adv. Mater.*, 2018, **30**, e1800075.
64 X. Li, C. Jiang, F. Zhao, L. Lan, Y. Yao, Y. Yu, J. Ping and Y. Ying, *Nano Energy*, 2019, **61**, 78–85.
65 M. Zhu, M. Lou, J. Yu, Z. Li and B. Ding, *Nano Energy*, 2020, **78**, 105208.
66 F. Jiang, X. Zhou, J. Lv, J. Chen, J. Chen, H. Kongcharoen, Y. Zhang and P. S. Lee, *Adv. Mater.*, 2022, **34**, e2200042.
67 S. Azimi, A. Golabchi, A. Nekookar, S. Rabbani, M. H. Amiri, K. Asadi and M. M. Abolhasani, *Nano Energy*, 2021, **83**, 105781.
68 S. Duan, J. Wu, J. Xia and W. Lei, *Sensors*, 2020, **20**, 2820.
69 Z. Li, M. Zhu, Q. Qiu, J. Yu and B. Ding, *Nano Energy*, 2018, **53**, 726–733.
70 H. Chen, L. Zhou, Z. Fang, S. Wang, T. Yang, L. Zhu, X. Hou, H. Wang and Z. L. Wang, *Adv. Funct. Mater.*, 2021, **31**, 2011073.
71 S. Gupta, R. Bhunia, B. Fatma, D. Maurya, D. Singh, Prateek, R. Gupta, S. Priya, R. K. Gupta and A. Garg, *ACS Appl. Energy Mater.*, 2019, **2**, 6364–6374.
72 T. Wang, K. Lu, Z. Xu, Z. Lin, H. Ning, T. Qiu, Z. Yang, H. Zheng, R. Yao and J. Peng, *Crystals*, 2021, **11**, 511.
73 L. Lee, K. H. Yoon, J. W. Jung, H. R. Yoon, H. Kim, S. H. Kim, S. Y. Song, K. S. Park and M. M. Sung, *Nano Lett.*, 2018, **18**, 5461–5466.
74 N. Sun, C. Jiang, Q. Li, D. Tan, S. Bi and J. Song, *J. Mater. Sci.: Mater. Electron.*, 2020, **31**, 20688–20729.
75 H. Kim, J. Park, S. Bak, J. Park, C. Byun, C. Oh, B. S. Kim, C. Han, J. Yoo, D. Kim, J. Song, P. Choi and B. Choi, *Sci. Rep.*, 2021, **11**, 21805.

76 F. Qiao, H. Chu, Y. Xie and Z. Weng, *Int. J. Energy Res.*, 2021, **46**, 4071–4087.
77 J. Tao, R. Wang, H. Yu, L. Chen, D. Fang, Y. Tian, J. Xie, D. Jia, H. Liu, J. Wang, F. Tang, L. Song and H. Li, *ACS Appl. Mater. Interfaces*, 2020, **12**, 9701–9709.
78 Y. Liu, L. Wang, L. Zhao, K. Yao, Z. Xie, Y. Zi and X. Yu, *Adv. Electron. Mater.*, 2020, **6**, 1901174.
79 W. Li, C. Li, G. Zhang, L. Li, K. Huang, X. Gong, C. Zhang, A. Zheng, Y. Tang, Z. Wang, Q. Tong, W. Dong, S. Jiang, S. Zhang and Q. Wang, *Adv. Mater.*, 2021, **33**, e2104107.
80 Z. Zhang, L. Weng, K. Guo, L. Guan, X. Wang and Z. Wu, *Ceram. Int.*, 2022, **48**, 4977–4985.
81 X. Zhou, L. Zhu, L. Fan, H. Deng and Q. Fu, *ACS Appl. Mater. Interfaces*, 2018, **10**, 31655–31663.
82 C. Lu, Z. Ji, G. Xu, W. Wang, L. Wang, Z. Han, L. Li and M. Liu, *Sci. Bull.*, 2016, **61**, 1081–1096.
83 A. Malik and B. Kandasubramanian, *Polym. Rev.*, 2018, **58**, 630–667.
84 B. Lu, Y. Wang, B.-R. Hyun, H.-C. Kuo and Z. Liu, *IEEE Electron Device Lett.*, 2020, 1040–1043, DOI: **10.1109/led.2020.2994143**.
85 Z. Zhang, L. Xia, L. Liu, Y. Chen, Z. Wang, W. Wang, D. Ma and Z. Liu, *J. Mater. Chem. C*, 2021, **9**, 2106–2114.
86 M. Qian, X. Mao, M. Wu, Z. Cao, Q. Liu, L. Sun, Y. Gao, X. Xuan, Y. Pan, Y. Niu and S. Gong, *Adv. Mater. Technol.*, 2021, **6**, 2100603.
87 B. Nie, X. Li, J. Shao, X. Li, H. Tian, D. Wang, Q. Zhang and B. Lu, *ACS Appl. Mater. Interfaces*, 2017, **9**, 40681–40689.
88 D. Qi, K. Zhang, G. Tian, B. Jiang and Y. Huang, *Adv. Mater.*, 2021, **33**, e2003155.
89 F. Li, Z. Xu, H. Hu, Z. Kong, C. Chen, Y. Tian, W. Zhang, W. Bin Ying, R. Zhang and J. Zhu, *Chem. Eng. J.*, 2021, **410**, 128363.
90 M. Chason, P. W. Brazis, Z. Jie, K. Kalyanasundaram and D. R. Gamota, *Proc. IEEE*, 2005, **93**, 1348–1356.
91 Q. Q. Afzal, K. Jaffar, M. Ans, J. Rafique, J. Iqbal, R. A. Shehzad and M. S. Mahr, *Polymer*, 2022, **238**, 18.
92 M. Song, D. S. You, K. Lim, S. Park, S. Jung, C. S. Kim, D. H. Kim, D. G. Kim, J. K. Kim, J. Park, Y. C. Kang, J. Heo, S. H. Jin, J. H. Park and J. W. Kang, *Adv. Funct. Mater.*, 2013, **23**, 4177–4184.
93 G. Zeng, J. W. Zhang, X. B. Chen, H. W. Gu, Y. W. Li and Y. F. Li, *Sci. China: Chem.*, 2019, **62**, 851–858.
94 K.-S. Choi, W. A. Braganca Jr, L. Jeong, K.-S. Jang, S. H. Moon, H. C. Bae, Y. S. Eom, M. K. Cho and S. I. Chang, *Presented in part at the 2018 IEEE 68th Electronic Components and Technology Conference (ECTC)*, 2018.
95 R. Get, S. M. Islam, S. Singh and P. Mahala, *Microelectron. Eng.*, 2020, **222**, 111200.
96 P. Wan, X. Wen, C. Sun, B. K. Chandran, H. Zhang, X. Sun and X. Chen, *Small*, 2015, **11**, 5409–5415.
97 W. S. Chang, T. S. Chang, C. M. Wang and W. S. Liao, *ACS Appl. Mater. Interfaces*, 2022, 22826–22837, DOI: **10.1021/acsami.1c20931**.
98 Y. Liu, J. Guo, J. Wang, X. Zhu, D. Qi, W. Li and K. Shen, *Eur. Polym. J.*, 2020, **125**, 109526.
99 X. Wu, C. Shu, X. He, S. Wang, X. Fan, Z. Yu, D. Yan and W. Huang, *Macromol. Chem. Phys.*, 2020, **221**, 1900506.
100 C. K. Chen, Y. C. Lin, L. C. Hsu, J. C. Ho, M. Ueda and W.-C. Chen, *ACS Sustainable Chem. Eng.*, 2021, **9**, 3278–3288.
101 S. Miyane, C. K. Chen, Y. C. Lin, M. Ueda and W. C. Chen, *ACS Appl. Polym. Mater.*, 2021, **3**, 3153–3163.
102 V. Khayrudinov, M. Remennyi, V. Raj, P. Alekseev, B. Matveev, H. Lipsanen and T. Haggren, *ACS Nano*, 2020, **14**, 7484–7491.
103 X. Wang, J. Li, H. Song, H. Huang and J. Gou, *ACS Appl. Mater. Interfaces*, 2018, **10**, 7371–7380.
104 B. You, C. J. Han, Y. Kim, B.-K. Ju and J.-W. Kim, *J. Mater. Chem. A*, 2016, **4**, 10435–10443.
105 C. Wu, X. Tang, L. Gan, W. Li, J. Zhang, H. Wang, Z. Qin, T. Zhang, T. Zhou, J. Huang, C. Xie and D. Zeng, *ACS Appl. Mater. Interfaces*, 2019, **11**, 20535–20544.
106 A. Lamberti, S. L. Marasso and M. Cocuzza, *RSC Adv.*, 2014, **4**, 61415–61419.
107 Q. Gao, Y. Pan, G. Zheng, C. Liu, C. Shen and X. Liu, *Adv. Compos. Hybrid Mater.*, 2021, **4**, 274–285.
108 X. Li, J. Yang, W. Yuan, P. Ji, Z. Xu, S. Shi, X. Han, W. Niu and F. Yin, *Compos. Commun.*, 2021, **23**, 100586.
109 M. H. Behfar, D. D. Vito, A. Korhonen, D. Nguyen, B. M. Amin, T. Kurkela, M. Tuomikoski and M. Mantysalo, *IEEE Trans. Compon., Packag., Manuf. Technol.*, 2021, **11**, 1022–1027.
110 W. B. Ying, H. Liu, P. Gao, Z. Kong, H. Hu, K. Wang, A. Shen, Z. Jin, L. Zheng, H. Guo, R. Zhang and J. Zhu, *Chem. Eng. J.*, 2021, **420**, 127691.
111 C. Ge, G. Wang, X. Li, J. Chai, B. Li, G. Wan, G. Zhao and G. Wang, *Compos. Sci. Technol.*, 2020, **197**, 108247.
112 S. Li, M. Liu, X. Zhou, Y. Dong and J. Li, *Macromol. Mater. Eng.*, 2021, **306**, 2000684.
113 S. Yoon, Y. J. Kim, Y. R. Lee, N.-E. Lee, Y. Won, S. Gandla, S. Kim and H.-K. Kim, *NPG Asia Mater.*, 2021, **13**, 13–14.
114 Y. Xiao, M. Wang, Y. Li, Z. Sun, Z. Liu, L. He and R. Liu, *Micromachines*, 2021, **12**, 1505.
115 Z. Li, R. Zhang, K.-S. Moon, Y. Liu, K. Hansen, T. Le and C. P. Wong, *Adv. Funct. Mater.*, 2013, **23**, 1459–1465.
116 J. Liu, P. Zhang, H. Wei, Z. Lu and Y. Yu, *Adv. Funct. Mater.*, 2021, **32**, 2107732.
117 J. Dou, L. Tang, L. Mou, R. Zhang and X. Jiang, *Compos. Sci. Technol.*, 2020, **197**, 108237.
118 Y. Su, Y. Zhao, H. Zhang, X. Feng, L. Shi and J. Fang, *J. Mater. Chem. C*, 2017, **5**, 573–581.
119 Y. Wang, Y. Yu, J. Guo, Z. Zhang, X. Zhang and Y. Zhao, *Adv. Funct. Mater.*, 2020, **30**, 2000151.
120 K. Batra, N. Sinha and B. Kumar, *Vacuum*, 2021, **191**, 110385.
121 J. Chen, Q. Yu, X. Cui, M. Dong, J. Zhang, C. Wang, J. Fan, Y. Zhu and Z. Guo, *J. Mater. Chem. C*, 2019, **7**, 11710–11730.
122 D. P. Jena, S. Anwar, R. K. Parida, B. N. Parida and N. C. Nayak, *J. Appl. Polym. Sci.*, 2021, **139**, 51743.
123 L. Ling, F. Liu, J. Li, G. Zhang, R. Sun and C.-P. Wong, *Macromol. Chem. Phys.*, 2018, **219**, 1800369.

124 F. Wang, Y. Tan, H. Peng, F. Meng and X. Yao, *Mater. Lett.*, 2021, **303**, 130512.
125 P. Ghahramani, K. Behdinan, R. Moradi-Dastjerdi and H. E. Naguib, *Nanotechnol. Rev.*, 2021, **11**, 55–64.
126 Y. Tang, Z. Zhao, H. Hu, Y. Liu, X. Wang, S. Zhou and J. Qiu, *ACS Appl. Mater. Interfaces*, 2015, **7**, 27432–27439.
127 S. Feng, H. Zhang, D. He, Y. Xu, A. Zhang, Y. Liu and J. Bai, *Energy Technol.*, 2019, **7**, 1900101.
128 X. Zhao, F. Meng and Y. Peng, *Composites, Part B*, 2022, **229**, 109466.
129 Y. Zhu, X. Chen, K. Chu, X. Wang, Z. Hu and H. Su, *Sensors*, 2022, **22**, 628.
130 K. Jeronimo, V. Koutsos, R. Cheung and E. Mastropaolo, *Sensors*, 2021, **21**, 5873.
131 I. Bozyel, Y. I. Keser and D. Gokcen, *Sens. Actuators, A*, 2021, **332**, 113056.
132 Y. Xu, X. Xie, H. Huang, Y. Wang, J. Yu and Z. Hu, *J. Mater. Sci.*, 2020, **56**, 2296–2310.
133 K. Zhou, Y. Zhao, X. Sun, Z. Yuan, G. Zheng, K. Dai, L. Mi, C. Pan, C. Liu and C. Shen, *Nano Energy*, 2020, **70**, 104546.
134 K. Ke, M. McMaster, W. Christopherson, K. D. Singer and I. Manas-Zloczower, *Composites, Part A*, 2019, **126**, 105614.
135 W. Li, Y. Zhou, Y. Wang, L. Jiang, J. Ma, S. Chen and F. L. Zhou, *Adv. Electron. Mater.*, 2020, **7**, 2000865.
136 X. Wang, S. Meng, M. Tebyetekerwa, Y. Li, J. Pionteck, B. Sun, Z. Qin and M. Zhu, *Composites, Part A*, 2018, **105**, 291–299.
137 S. Choi, S. I. Han, D. Jung, H. J. Hwang, C. Lim, S. Bae, O. K. Park, C. M. Tschabrunn, M. Lee, S. Y. Bae, J. W. Yu, J. H. Ryu, S. W. Lee, K. Park, P. M. Kang, W. B. Lee, R. Nezafat, T. Hyeon and D. H. Kim, *Nat. Nanotechnol.*, 2018, **13**, 1048–1056.
138 M. Park, J. Im, M. Shin, Y. Min, J. Park, H. Cho, S. Park, M. B. Shim, S. Jeon, D. Y. Chung, J. Bae, J. Park, U. Jeong and K. Kim, *Nat. Nanotechnol.*, 2012, **7**, 803–809.
139 S. Badatya, D. K. Bharti, N. Sathish, A. K. Srivastava and M. K. Gupta, *ACS Appl. Mater. Interfaces*, 2021, **13**, 27245–27254.
140 H. Cheraghi Bidsorkhi, A. G. D'Aloia, A. Tamburrano, G. De Bellis and M. S. Sarto, *Sensors*, 2021, **21**, 5277.
141 S. Ippili, V. Jella, A. M. Thomas, C. Yoon, J.-S. Jung and S.-G. Yoon, *J. Mater. Chem. A*, 2021, **9**, 15993–16005.
142 G. Y. Li, J. Li, Z. J. Li, Y. P. Zhang, X. Zhang, Z. J. Wang, W. P. Han, B. Sun, Y. Z. Long and H. D. Zhang, *Adv. Compos. Hybrid Mater.*, 2021, **5**, 766–775.
143 X. Hu, Z. Ding, L. Fei, Y. Xiang and Y. lin, *J. Mater. Sci.*, 2019, **54**, 6401–6409.
144 S. M. S. Rana, M. T. Rahman, M. Salauddin, S. Sharma, P. Maharjan, T. Bhatta, H. Cho, C. Park and J. Y. Park, *ACS Appl. Mater. Interfaces*, 2021, **13**, 4955–4967.
145 K. Shi, B. Sun, X. Huang and P. Jiang, *Nano Energy*, 2018, **52**, 153–162.
146 M. Zhu, M. Lou, I. Abdalla, J. Yu, Z. Li and B. Ding, *Nano Energy*, 2020, **69**, 104429.
147 R. Sahoo, S. Mishra, A. Ramadoss, S. Mohanty, S. Mahapatra and S. K. Nayak, *Polymer*, 2020, **205**, 122869.
148 Y. Kim, X. Wu, C. Lee and J. H. Oh, *ACS Appl. Mater. Interfaces*, 2021, **13**, 36967–36975.
149 A. Ahmed, Y. Jia, H. Deb, M. F. Arain, H. Memon, K. Pasha, Y. Huang, Q. Fan and J. Shao, *J. Mater. Sci.: Mater. Electron.*, 2022, **33**, 3965–3981.
150 S. Yu, Y. Zhang, Z. Yu, J. Zheng, Y. Wang and H. Zhou, *Nano Energy*, 2021, **80**, 105519.
151 H. Li, W. Lian, T. Cheng, W. Zhang, B. Lu, K. Tan, C. Liu and C. Shen, *ACS Sustainable Chem. Eng.*, 2021, **9**, 17128–17141.
152 X. Gao, M. Zheng, X. Yan, J. Fu, M. Zhu and Y. Hou, *J. Mater. Chem. C*, 2019, **7**, 961–967.
153 P. Snapp, C. Cho, D. Lee, M. F. Haque, S. Nam and C. Park, *Adv. Mater.*, 2020, **32**, e2004607.
154 H. J. Kim, M. Y. Lee, J. S. Kim, J. H. Kim, H. Yu, H. Yun, K. Liao, T. S. Kim, J. H. Oh and B. J. Kim, *ACS Appl. Mater. Interfaces*, 2017, **9**, 14120–14128.
155 I. A. Rashid, M. S. Irfan, Y. Q. Gill, R. Nazar, F. Saeed, A. Afzal, H. Ehsan, A. A. Qaiser and A. Shakoor, *Polym. Bull.*, 2019, **77**, 1081–1093.
156 M. Wang, P. Baek, A. Akbarinejad, D. Barker and J. Travas-Sejdic, *J. Mater. Chem. C*, 2019, **7**, 5534–5552.
157 M. Amirkhosravi, L. Yue and I. Manas-Zloczower, *ACS Appl. Polym. Mater.*, 2020, **2**, 4037–4044.
158 Y. Ding, W. Xu, W. Wang, H. Fong and Z. Zhu, *ACS Appl. Mater. Interfaces*, 2017, **9**, 30014–30023.
159 Y. Wang, Z. Yu, G. Mao, Y. Liu, G. Liu, J. Shang, S. Qu, Q. Chen and R.-W. Li, *Adv. Mater. Technol.*, 2019, **4**, 1800435.
160 S. Zhu, H. Sun, Y. Lu, S. Wang, Y. Yue, X. Xu, C. Mei, H. Xiao, Q. Fu and J. Han, *ACS Appl. Mater. Interfaces*, 2021, **13**, 59142–59153.
161 N. Johner, C. Grimaldi, I. Balberg and P. Ryser, *Phys. Rev. B: Condens. Matter Mater. Phys.*, 2008, **77**, 11.
162 S. Holliday, R. S. Ashraf, A. Wadsworth, D. Baran, S. A. Yousaf, C. B. Nielsen, C. H. Tan, S. D. Dimitrov, Z. Shang, N. Gasparini, M. Alamoudi, F. Laquai, C. J. Brabec, A. Salleo, J. R. Durrant and I. McCulloch, *Nat. Commun.*, 2016, **7**, 11585.
163 K. G. Cho, H. J. Kim, H. M. Yang, K. H. Seol, S. J. Lee and K. H. Lee, *ACS Appl. Mater. Interfaces*, 2018, **10**, 40672–40680.
164 F. De Rossi, G. Renno, B. Taheri, N. Yaghoobi Nia, V. Ilieva, A. Fin, A. Di Carlo, M. Bonomo, C. Barolo and F. Brunetti, *J. Power Sources*, 2021, **494**, 229735.
165 S. Lee, H. Kim and Y. Kim, *Electronics*, 2021, **10**, 2283.
166 S. Lee, H. Kim and Y. Kim, *ACS Appl. Polym. Mater.*, 2022, **4**, 6817–6824.
167 Y. H. Kim, C. Sachse, M. L. Machala, C. May, L. Müller-Meskamp and K. Leo, *Adv. Funct. Mater.*, 2011, **21**, 1076–1081.
168 H. Xu, X. Zhao, G. Yang, X. Ji, X. Zhang, L. Li, B. Wu, X. Ouyang, Y. Ni, L. Chen and H.-C. Hu, *Chem. Eng. J.*, 2022, **430**, 133014.
169 X. Fan, B. Xu, N. Wang, J. Wang, S. Liu, H. Wang and F. Yan, *Adv. Electron. Mater.*, 2017, **3**, 1600471.

170 Y. Song, T.-Y. Liu, X.-X. Xu, D.-Y. Feng, Y. Li and X.-X. Liu, *Adv. Funct. Mater.*, 2015, **25**, 4626–4632.
171 M. Vosgueritchian, D. J. Lipomi and Z. Bao, *Adv. Funct. Mater.*, 2012, **22**, 421–428.
172 W. Li, Y. Zhou, Y. Wang, L. Jiang, J. Ma, S. Chen and F. L. Zhou, *Adv. Electron. Mater.*, 2020, **7**, 2000865.
173 A. C. Hinckley, S. C. Andrews, M. T. Dunham, A. Sood, M. T. Barako, S. Schneider, M. F. Toney, K. E. Goodson and Z. Bao, *Adv. Electron. Mater.*, 2021, **7**, 2001190.
174 U. Lang, N. Naujoks and J. Dual, *Synth. Met.*, 2009, **159**, 473–479.
175 X. Jing, Z. Ma, M. F. Antwi-Afari, L. Wang, H. Li, H.-Y. Mi, P.-Y. Feng and Y. Liu, *Ind. Eng. Chem. Res.*, 2021, **60**, 10419–10430.
176 S. M. Mirmohammadi, S. Hoshian, V. P. Jokinen and S. Franssila, *Sci. Rep.*, 2021, **11**, 12646.
177 L. Wang, J. Luo, Y. Chen, L. Lin, X. Huang, H. Xue and J. Gao, *ACS Appl. Mater. Interfaces*, 2019, **11**, 17774–17783.
178 R. Zhang, S. Li, C. Ying, Z. Hu, A. Lv, H. Hu, X. Fu, S. Hu, Q. Liu and C.-P. Wong, *Compos. Sci. Technol.*, 2020, **200**, 108319.
179 S. J. Paul, I. Elizabeth and B. K. Gupta, *ACS Appl. Mater. Interfaces*, 2021, **13**, 8871–8879.
180 S. Kumar, T. K. Gupta and K. M. Varadarajan, *Composites, Part B*, 2019, **177**, 107285.
181 Y. Wang, J. Hao, Z. Huang, G. Zheng, K. Dai, C. Liu and C. Shen, *Carbon*, 2018, **126**, 360–371.
182 W. Zhai, J. Zhu, Z. Wang, Y. Zhao, P. Zhan, S. Wang, G. Zheng, C. Shao, K. Dai, C. Liu and C. Shen, *ACS Appl. Mater. Interfaces*, 2022, **14**, 4562–4570.
183 X. W. Wang, Y. Gu, Z. P. Xiong, Z. Cui and T. Zhang, *Adv. Mater.*, 2014, **26**, 1336–1342.
184 S. Cho, J. H. Song, M. Kong, S. Shin, Y. T. Kim, G. Park, C. G. Park, T. J. Shin, J. Myoung and U. Jeong, *ACS Appl. Mater. Interfaces*, 2017, **9**, 44096–44105.
185 S. Luo, X. Zhou, X. Tang, J. Li, D. Wei, G. Tai, Z. Chen, T. Liao, J. Fu, D. Wei and J. Yang, *Nano Energy*, 2021, **80**, 105580.
186 S. Zhao, W. Ran, D. Wang, R. Yin, Y. Yan, K. Jiang, Z. Lou and G. Shen, *ACS Appl. Mater. Interfaces*, 2020, **12**, 32023–32030.
187 J. Hwang, Y. Kim, H. Yang and J. H. Oh, *Composites, Part B*, 2021, **211**, 108607.
188 Q. Zhang, F. Gao, C. Zhang, L. Wang, M. Wang, M. Qin, G. Hu and J. Kong, *Compos. Sci. Technol.*, 2016, **129**, 93–100.
189 M. N. Tchoul, S. P. Fillery, H. Koerner, L. F. Drummy, F. T. Oyerokun, P. A. Mirau, M. F. Durstock and R. A. Vaia, *Chem. Mater.*, 2010, **22**, 1749–1759.
190 X. Fu, J. Zhang, J. Xiao, Y. Kang, L. Yu, C. Jiang, Y. Pan, H. Dong, S. Gao and Y. Wang, *Nanoscale*, 2021, **13**, 18780–18788.
191 J. Wang, Y. Lou, B. Wang, Q. Sun, M. Zhou and X. Li, *Sensors*, 2020, **20**, 2459.
192 A. Chhetry, S. Sharma, H. Yoon, S. Ko and J. Y. Park, *Adv. Funct. Mater.*, 2020, **30**, 1910020.